5-2012

An Investigation into Delta Wing Vortex Generators as a Means of Increasing Algae Biofuel Raceway Vertical Mixing Including an Analysis of the Resulting Turbulence Characteristics

Aaron H. Godfrey
Utah State University

AN INVESTIGATION INTO DELTA WING VORTEX GENERATORS AS A MEANS OF INCREASING ALGAE BIOFUEL RACEWAY VERTICAL MIXING INCLUDING AN ANALYSIS OF THE RESULTING TURBULENCE CHARACTERISTICS

by

Aaron H. Godfrey

A thesis submitted in partial fulfillment
of the requirements for the degree

of

MASTER OF SCIENCE

in

Mechanical Engineering

Approved:

Byard Wood Co-Major Professor	Robert Spall Co-Major Professor
Ronald Sims Committee Member	Mark R. McLellan Vice President for Research and Dean of the School of Graduate Studies

UTAH STATE UNIVERSITY
Logan, Utah

2012

ABSTRACT

An Investigation into Delta Wing Vortex Generators as a Means of Increasing Algae Biofuel Raceway Vertical Mixing Including an Analysis of the Resulting Turbulence Characteristics

by

Aaron H. Godfrey, Master of Science

Utah State University, 2012

Major Professors: Dr. Byard Wood and Dr. Robert Spall
Department: Mechanical and Aerospace Engineering

Algae-derived biodiesel is currently under investigation as a suitable alternative to traditional fossil-fuels. Though it possesses many favorable characteristics, algae remains prohibitively expensive to mass produce and distribute. The most economical means of growing algae are large-scale open pond raceways. These, however, suffer from low culture densities; this fact impacts the cost directly through diminished productivity, as well as indirectly by raising costs due to the necessity of dewatering low culture density raceway effluent. Algae, as a photosynthetic organism, achieves higher culture densities when sufficient light is provided. In open ponds this can be accomplished by frequently cycling algae to the raceway surface. The current work examined delta wing vortex generators as a means of instigating this cycling motion. In particular the impact of spacing and angle of attack was analyzed. These vortex generators were found to significantly increase vertical mixing when placed in a series,

developing precisely the motion desired. Their impact on power requirements was also examined. Specifically it was shown that increases in spacing and decreases in angle of attack result in lower power consumption. It was demonstrated that the most efficient mixing generation is achieved by larger spacings and smaller angles of attack. The impact that these devices had on raceway turbulence as measured by dissipation rate was also investigated and compared to published values for algae growth. Raceways were found to be significantly more turbulent than standard algae environments, and adding delta wings increased these levels further.

(81 pages)

PUBLIC ABSTRACT

Aaron H. Godfrey, Master of Science

Utah State University, 2012

Major Professors: Dr. Byard Wood and Dr. Robert Spall
Department: Mechanical and Aerospace Engineering

Current standards of living and future prosperity are closely tied to the availability of sufficient and inexpensive energy resources. Currently society is fueled primarily by some form of fossil fuel. By their very nature these fuel sources are non-renewable, thus our current energy habits are unsustainable. Among the various renewable energy technologies is the capability to produce diesel fuel by colonies of algae. While this technology has many positive features it remains too expensive to be a realistic fuel source. The current work performed analysis using computer simulation of an aquatic environment commonly used to grow algae for the purposes of harvesting diesel fuel in order to identify design opportunities that would lead to higher productivities, having the impact of lowering the fuel costs. It was found that minor alterations to these environments produce mixing that is expected to increase algae growth with a limited impact on the operational costs of a fuel production facility. These results have the benefit of providing insight and direction into how we might plausible lower algae diesel costs. The cost associated with this research was entirely the result of personnel, software, and hardware costs having a combined expense of approximately $50,000.

ACKNOWLEDGMENTS

I am grateful for all those who contributed to this work, including my committee and co-workers. I would like to specifically thank and recognize a few without whom I would never have accomplished the task.

I am deeply grateful for the influence and blessings of an all merciful God and His Son Jesus Christ. Having been created in their image and received from them the very modest intellectual abilities which I possess, it was they who enabled me to accomplish this task. I hope that my efforts might in part fulfill the injunction, “Wisdom is the principal thing; therefore get wisdom: and with all thy getting get understanding.”

I wish to thank Dr. Robert Spall for the many hours of advice and help he offered me as I muddled my way through this project. There is no exaggeration in stating that without his help I would never have finished. It was he who introduced me to CFD and found this opportunity for me. In so doing he changed the course of my professional life.

I would like to thank Dr. Byard Wood for trusting me with this project, allocating the funding necessary for its completion, and mentoring me along the way.

Many other individuals provided invaluable service including Denver Smith and Jon Huppi from the Center for High Performance Computing.

I am most grateful for the loving support and example of my wife, Valerie. She has been an inspiration and balm to me during these last several years. She represents the very best there is in my life, and was always there to encourage me when I doubted my abilities to perform at the level necessary to complete this degree. I love you, Sweetheart.

Aaron Harrison Godfrey

CONTENTS

LIST OF TABLES

LIST OF FIGURES

NOMENCLATURE

f_w	Wall-damping function
f_{v1}	Wall-damping function
f_{v2}	Wall-damping function
k	Turbulent kinetic energy per unit mass ($m^2\ s^{-2}$)
t	Time (s)
u_1'	Fluctuating velocity component in the x_1 direction ($m\ s^{-1}$)
u_2'	Fluctuating velocity component in the x_2 direction ($m\ s^{-1}$)
u_3'	Fluctuating velocity component in the x_3 direction ($m\ s^{-1}$)
u^+	Dimensionless Turbulence wall velocity
y	Distance from nearest wall
y^+	Dimensionless Turbulent wall distance
B	Law of the wall additive constant (5.0)
C_{b1}	Spalart-Allmaras turbulence model constant (0.1355)
C_{b2}	Spalart-Allmaras turbulence model constant (0.622)
C_{w1}	Spalart-Allmaras turbulence model constant (7.1)
C_μ	Standard k-ε model constant
M_I	Vertical mixing intensity
P	Mean pressure term (Pa)
P_r	System power requirement (W)
P_s	Mass specific power requirement (W/kg)
Q	Volumetric flow rate ($m^3\ s^{-1}$)

S_{ij}	Deformation rate tensor (s^{-1})
SΦ	Passive scalar source term (m^{-3})
U_1	Mean velocity component in the x_1 direction ($m\ s^{-1}$)
U_2	Mean velocity component in the x_2 direction ($m\ s^{-1}$)
U_3	Mean velocity component in the x_3 direction ($m\ s^{-1}$)
V	Raceway or channel volume (m^3)
$\overline{V}$	Average channel or raceway velocity ($m\ s^{-1}$)
β*	k-ω SST turbulence model constant
β_2	k-ω SST turbulence model constant
γ_2	k-ω SST turbulence model constant
δ_{ij}	Kronecker delta
ε	Turbulence dissipation rate per unit mass ($m^2\ s^{-3}$)
κ	Von Karman's law of the wall constant (0.42)
κ_{sa}	Spalart-Allmaras turbulence model constant (0.41)
μ	Dynamic viscosity ($kg\ m^{-1}\ s^{-1}$)
μ_t	Turbulent eddy viscosity ($kg\ m^{-1}\ s^{-1}$)
ν	Kinematic viscosity ($m^2\ s^{-1}$)
$\tilde{\nu}$	Kinematic eddy viscosity parameter ($m^2\ s^{-1}$)
ρ	Fluid density ($kg\ m^{-3}$)
σ_k	k-ω SST turbulence model constant
σ_v	Spalart-Allmaras turbulence model constant (0.666)
$\sigma_{\omega,1}$	k-ω SST turbulence model constant
$\sigma_{\omega,2}$	k-ω SST turbulence model constant

φ'	Fluctuating passive scalar concentration per unit mass (kg^{-1})
ω	Turbulence frequency (s^{-1})
Γ_Φ	Diffusion coefficient of passive scalar ($m^{-1}\ s^{-1}$)
Δp	Pressure drop (Pa)
$\Delta\Phi$	Passive scalar percent difference from initial concentration difference
$\Delta\Phi_0$	Passive scalar initial concentration difference
Φ	Mean passive scalar concentration
$\overline{\Phi}$	Raceway mass averaged passive scalar concentration
Ω_{ij}	Mean Vorticity tensor

CHAPTER 1

INTRODUCTION

Fossil fuel energy requirements continue to be a topic of significant debate both domestically as well as globally. A particular source of controversy is the world's ever quickening pace of fuel consumption. Core causes of this acceleration are a combination of increases in demand from developed countries as well as the rapid growth in demand from nations that are transitioning onto the world stage as new market powers such as China, Brazil, Russia, and India. The continued use, and in particular accelerating use, of fossil fuel energy sources is meeting significant reticence from the global community. This reticence is the result of three major concerns: 1) the unsustainable nature of these resources, 2) the dependence upon politically unstable regions of the world for their supply, and 3) concerns over their impact on the global climate [1].

These concerns have served as the impetus for advanced research into alternative forms of energy. Researchers from institutions across the globe are investigating new and advanced energy technologies such as wind, solar, tidal, and nuclear to name a few. Among the many technologies being considered is the production of biologically derived fuels (biofuels). Though this technology is applied in many different ways the core principles are the same. Either a biological carbon source or CO_2 (in photosynthetic systems) is used to sustain either a chemical or biological process that captures energy from the carbon source (sunlight in photosynthetic systems) and stores it in the form of a liquid or gaseous fuel with many similarities to those derived from fossil fuels (e.g. oil, gasoline, or natural gas).

The number of carbon sources under consideration in research or industry is significant and only a few are named here (corn, soybean, canola flowers, and coconut). Numerous differences in economics, scalability, resource management, and thermodynamics exist between these technologies. Among the many concerns is the impact of consuming significant amounts of the carbon source for fuel generation on global food prices [2]. The impact can be seen as a consequence of direct competition (corn) and/or competition for agricultural land (canola flowers).

The subject of the current work relates directly to a technology that is being developed in response to these concerns, that of algae derived biodiesel. When compared to competing forms of biofuels algae biodiesel (ABD) has several important advantages. In particular algae is well suited to non-arable land, requires significantly less total land for the same volume of fuel, requires less water than terrestrial crops, experiences exponential growth rates, doesn't compete with food crops, and doesn't require the use of potentially harmful pesticides [3]. In addition to these benefits this technology has significant advantages as a source of energy when considered from the perspective of the three concerns referenced in the introductory paragraph: sustainability, environmental, and political stability [2].

Our current understanding of algae suggests two manners in which hydrodynamics have the potential to impact algae growth. First, as algae are in most cases a nearly neutrally buoyant organism grown in aqueous culture their relative position in a raceway is principally determined by hydrodynamics. This has significant implications for algae as a photosynthetic organism. Algae located near the surface of an open raceway pond will have significantly more favorable access to light than algae that

is located in the lower extents of the raceway. Thus a hydrodynamic environment which permitted algae to cycle from the bottom of the raceway to the light rich surface would provide more homogeneous access to light. This implies that the presence of vertical mixing in the environment used to grow algae may improve growth conditions and productivities. The second anticipated impact of the flow regime on algae growth is the result of the well-established relationship between the level of environmental turbulence and algae growth. Addition of vortex generators is anticipated to increase the levels of turbulence present in the growth environment.

The above considerations imply an opportunity for improved ABD production based on engineering of the hydrodynamic environment. It is anticipated that improving sunlight availability by means of vertical mixing in conjunction with strain selection of organisms that are more robust to environmental turbulence could result in higher growth densities in open raceways. As will be seen in the literature review this fact has a real and significant impact of the economics of ABD production.

The research presented here-in investigates the impact of vortex generation devices on pilot scale algae raceways under investigation by Utah State University's BioEnergy Center. In particular the levels of vertical mixing, presence of turbulence (as indicated by values of turbulence dissipation rate ε), and the impact that vortex generation has on system power requirements was investigated by means of computational fluid dynamics (CFD) simulations.

The intent of this project was to determine the impact of delta wing vortex generation devices (DWVGs) on algae raceway vertical mixing and turbulence. Of particular interest was the effect of these DWVGs on the power required to maintain

raceway circulation. It was hypothesized at the outset of this research that introduction of DWVGs represents a viable means of achieving increases in vertical mixing and turbulence while having a minor impact on the power requirements, creating opportunities for more economically viable ABD production as a result.

The remainder of this thesis will be dedicated to the development of the necessary literature review to understand the proposed goals as well as the hypothesis that was investigated. In particular the published literature pertaining to the current state of the art of ABD production, turbulence on algae growth, and mixing generation technology will be outlined. Following the literature review the methods employed to investigate the hypothesis as well as those required to determine that the outcome was sufficiently sound are presented. Finally the results are presented and analyzed and conclusions are drawn and discussed.

CHAPTER 2

LITERATURE REVIEW

2.1 Algae Biodiesel Economics

Notwithstanding the advantages of algal biodiesel, large scale implementation of this technology has many remaining challenges. Nearly all of these challenges stem from the fact that in the current environment algae produced biodiesel is not economically competitive with fossil fuels [2,4]. Proponents of this technology advocate an array of strategies for closing the gap, including: government subsidies, development of secondary high value products (HVPs), joint bio-methane production, and continued research into improving the technology's efficiency and thus economics [2,4,5].

While it is likely a reality that the future of the ABD industry will depend on a combination of these techniques the first two present several challenges. Given the current economic state of affairs of most developed nations it may not be politically feasible or indeed desirable to implement subsidies on the scale required to make ABD viable. In the case of the HVP manufacturing there are inherent differences in the scales of fuel markets and any market for which a HVP might be developed. Fuel is in nature a very large market with a low product cost when compared to the markets for proteins for example. This leads to completely different economies of scale. One researcher estimated that including governmental credits and proceeds from sales of a secondary product of the production process (glycerin) resulted in a net cost reduction of less than 3% [4]. Bio-methane is generally seen as a viable means of impacting the economics of ABD, however this alone will not resolve all problems. Thus it is essential that the

processes involved in the generation of ABD be continually studied in order to make them more efficient.

This reality has resulted in a deluge of research (and consequently funding) resources to address the perceived inefficiencies of algal photosynthetic energy capture systems in an effort to make them economically viable. For a thorough review of the difficulties and current approaches to overcome them the reader is referred to two excellent reviews: those of Mata et al. [6] and Christenson and Sims [7].

A significant cost driver in the process of generating ABD comes as a result of the expense of concentrating the algae prior to the final step of converting bio-lipids to diesel fuel. Grown in aqueous culture algae are often dilute, on the order of 0.02% – 0.06% total suspended solids (TSS), lipid to fuel conversion typically requires an algal cake composed of around 15% - 25% TSS [8]. Dewatering, the step where dilute algal solutions are concentrated sufficiently for bio-diesel conversion, has been identified as the second most costly step in the ABD production process [4]. Thus improvements in this step represent a significant opportunity for improving the economic viability of ABD as a whole.

2.2 Algae Sensitivity to Environmental Turbulence

The impact of turbulence on micro-algae growth has been demonstrated by several researchers. Early researchers observed this relationship in natural environments or in laboratory cultures being prepared for different studies [9,10]. As the existence of a relationship between turbulence and algae growth became accepted researchers began formal experimentation in an attempt to better understand this phenomena. Many of the earliest studies employed unrealistically simply devices to expose the algae to turbulence

such as shaker flasks and Couette cylinders [11-14], which led to a generally accepted axiom that turbulence is inhibitory to algae growth. Recent studies have applied more sophisticated and realistic turbulence generation methods in conjunction with more advanced turbulence measurement and quantification techniques. The findings of a few of these studies are presented below.

Sullivan and Swift [15] in 2003 completed one of the most thorough studies on the impact of turbulence to date. It their paper they sought to test what had become a generally accepted paradigm; that environmental turbulence had an inhibitory impact on algae growth. To evaluate the accuracy of this paradigm the authors subjected 10 different species of autotrophic marine dino-flagellates to varying levels of quantified three-dimensional turbulence. The species were carefully selected for their morphological and physiological diversity; in addition two species were selected because of the existence of previously published research regarding their sensitivity to turbulence.

Turbulence was generated by means of a vertical oscillating pair of 2.5 cm rods. In order to quantify the turbulence generated an acoustic Doppler velocimeter (ADV) was employed to measure the turbulence dissipation rate ε. The authors selected three different experimental conditions: a high level of turbulence ($\varepsilon = 10^{-4}$ m^2s^{-3}), a low level of turbulence ($\varepsilon = 10^{-8}$ m^2s^{-3}), and stagnant or no turbulence. The levels of turbulence selected were representative of common conditions found in natural oceanic algal environments. The low level of turbulence represents conditions that are found to be on the lower to moderate end, while the high levels are more exceptional conditions that algae may encounter for example during a storm with significant surface wind mixing. The presence of low level turbulence was found to have no effect on any of the 10

species investigated. It was found that in the presence of high levels of turbulence, of the 10 species under investigation, four exhibited no significant impact, three were negatively impacted, and three were positively impacted. Interestingly enough it was also found that the two species chosen for comparison to previous research the results were contradictory. In both cases published literature had claimed turbulence would have an inhibitory effect, however, Sullivan and Swift found that in one case the species was unaffected and the other experienced enhanced growth in the presence of turbulence. The authors address this in their discussion, and it seems apparent that the methods used to generate the turbulence in the previous research may limit the potential for direct comparison to these results. In addition to this finding it is also significant that 30% of the species investigated actually experienced enhanced growth in the presence of high levels of turbulent motion. They conclude that no single paradigm is capable of usefully describing the complex relationship between turbulence and algae growth.

Another important study was completed by Warnarrs and Hondzo [16] in 2006, in which they investigated in detail the impact that three-dimensional turbulence had on a single algal species. They investigated growth rate as well as nutrient uptake. Turbulence generation was accomplished through the means of submersible speakers placed on opposing sides of a rectangular Plexiglas chamber, each with a solid grid placed in front to generate small scale eddies. The speakers were fed out of phase sin wave signals, which had the effect of intermittently propelling water from one side to the other. This set up was particularly designed to mimic turbulence that is common in lakes and oceans, and as such it had no moving parts.

Turbulence quantification was performed by means of particle image velocimetry (PIV). The frequency and voltage were varied in order to change the levels of ε in the chamber. For the cases of lower ε it was shown that the turbulence was very isotropic in nature, while for the higher ε cases distinct non-isotropic spatial gradients were present. The range of ε investigated ranged from 10^{-9} m^2s^{-3} to 10^{-6} m^2s^{-3} representing very quiescent to moderately turbulent conditions.

It was found that under these conditions turbulence was shown to have a positive effect on the strain of algae selected. In fact a nearly two fold increase in growth rate was seen for the highest level of ε tested in the experiment. These results were again contradictory to previously published research cited in the article. The authors note primarily that the previous researchers exposed the algae to significantly higher values of ε.

The significance of these more current studies is that while turbulence continues to be recognized as an important factor in growing algae, it is now clear that this relationship is complex and species dependent. In many cases it can be seen that the impact of turbulence can be large and positive. While this can significantly impact the productivity of algae biofuel facility it remains a minor or uninvestigated subject in nearly all efforts to produce a feasible biofuel production facility.

2.3 Vertical Mixing Generation

Published literature supports the choice of delta wings as a viable means of vortex generation. In particular researchers interested in improving the heat transfer characteristics of tube heat exchangers have evaluated their capacity to generate

longitudinal streamwise vortices (LSVs) increase mixing and correspondingly convective heat transfer.

Early studies of importance both illustrated the vortex generation potential of delta wings as well as made important performance comparisons with other means of vortex generation. Fiebig et al. [17] in 1991 produced an important study wherein vortex generators of different geometries were investigated at multiple angles of attack to determine their impact on the local heat transfer coefficient as well as drag induced by their presence. They concluded that drag induced by vortex generators was a function of the projected area and not shape. Their results concluded that delta wing vortex generators (DWVGs) produced the highest heat transfer enhancement per vortex generator area. Tiggelbeck et al. [18] in 1994 have similarly concluded that delta wings or winglets present the best method of heat transfer enhancement.

Subsequent research sought to understand the mechanism that resulted in heat transfer enhancement. In 1996 the research of Biswas et al. [19], undertook to understand the impact of delta wing vortex generators on flow structure. They completed both experiment and numerical work which analyzed in detail the development of LSVs as a result of DWVGs. Gentry and Jacobi [20] in 2002 showed experimentally that the strength of the LSVs is a function of Reynolds number based on the chord length, angle of attack, and wing aspect ratio. An increase in any of these parameters was shown to increase vortex strength as well as heat transfer. The early work of Eibeck and Eaton [21] found that the influence of LSVs on momentum and energy transport could be identified at lengths of 60 delta wing chords downstream of the wing itself.

The results of these researchers form a strong basis for the selection of DWVG's as a means of generating vertical mixing in algae open channel raceways. In particular the flow structures shown to be induced by DWVGs are ideal for attempting to cycle algae between light surface and dark depths.

CHAPTER 3

CFD SIMULATION EQUATIONS AND RESOURCES

The detailed investigation of vertical mixing and turbulence present in algae raceways under consideration for biofuel production presents several modeling challenges. CFD represents a robust method for developing a model capable of yielding physically significant results. This chapter is devoted to the presentation of the governing equations employed for the CFD modeling and description of the resources utilized to complete the research. In it the governing equations that make up the model are presented, including basic background information, particularly in the case of turbulence modeling.

3.1 Governing Equations

3.1.1 Navier-Stokes Equations

Open channel flow such as that present in algae raceways can be modeled by the unsteady three-dimensional incompressible Navier-Stokes equations, which represent Newton's second law for a fluid element and are given in Eqn. (1) below in standard tensor notation [22]. They result in a set of coupled transport equations for the three components of linear momentum, and as such are often referred to as the momentum equations. The last equation is the incompressible conservation of mass or continuity equation.

$$\begin{aligned} &\frac{\partial u_i}{\partial t} + \frac{\partial (u_i u_j)}{\partial x_j} = -\frac{1}{\rho}\frac{\partial p}{\partial x_i} + \nu \frac{\partial^2 u_i}{\partial x_j^2} \\ &\frac{\partial u_i}{\partial x_i} = 0 \end{aligned} \tag{1}$$

3.1.2 Turbulence Models

For all fluid dynamics problems a flow characteristic of fundamental importance is whether the flow is characterized by turbulent (three-dimensional, unsteady chaotic motion) or laminar (no turbulence present) motion. Raceways of interest for algae production are characterized by turbulence. In such flows additional governing equations representing an appropriate turbulence model must be selected due to computational resource limitations that make direct simulation of the turbulent motion unfeasible.

The research presented here in will make use of turbulence models which are based on a Reynolds averaging of the Navier-Stokes equations, given in Eqn. (1) [22] in standard tensor notation. Reynolds averaging involves the decomposition of the field variables into average and fluctuating components; after transformation of the field variables into their decomposed components and application of statistical operations [22] on the mean and fluctuating terms Eqn. (2) is obtained.

$$\frac{\partial U_i}{\partial t} + \frac{\partial (U_i U_j)}{\partial x_j} = -\frac{1}{\rho}\frac{\partial P}{\partial x_i} + \nu \frac{\partial^2 U_i}{\partial x_j^2} + \frac{1}{\rho}\frac{\partial (\overline{u_i' u_j'})}{\partial x_j}$$
$$\frac{\partial U_i}{\partial x_i} = 0 \qquad (2)$$

This process accomplishes two things: first it transforms the Navier-Stokes equations from a set of transport equations for the individual velocity components to a set of transport equations for the mean values of the velocity components; secondly it produces an additional term known as the Reynolds stress. This term is also the cause of what is known as the turbulence closure problem. Equation (1) represents a closed system of four equations and four unknowns (three velocity components and pressure).

Equation (2), however, represents an unclosed system of four equations and 10 unknowns. Additional equations are required for solution. In particular a method for computing the Reynolds Stress terms is required.

There are two basic methods of providing closure. The first method which is not used in the current work is to develop a set of six additional transport equations, one for each of the Reynolds Stress terms. The second method is to define either a single equation or set of equations that govern the transport of gross turbulent properties. In addition a model is selected that equates these gross turbulent properties to the Reynolds stresses. There are several such methods available for use and two have been selected for the current work.

3.1.2.1 k-ω SST Model

Equation (3) represents one such model, the k-ω Shear Stress Transport (SST) model including the relationship that defines the Reynolds stress computations necessary to couple to Eqn. (2). In the case of the k-ω model this represents the well-known Boussinesq approximation [22]. This model attempts to define transport equations for the turbulent kinetic energy k and the specific dissipation rate ω.

$$\rho\frac{\partial k}{\partial t}+\rho\frac{\partial (kU_j)}{\partial x_j}=\frac{\partial}{\partial x_j}\left[\left(\mu+\frac{\mu_t}{\sigma_k}\right)\frac{\partial k}{\partial x_j}\right]+\left(2\mu_t S_{ij}S_{ij}-\frac{2}{3}\rho k\frac{\partial U_i}{\partial x_j}\delta_{ij}\right)$$
$$-\beta^*\rho k\omega$$
$$\rho\frac{\partial \omega}{\partial t}+\rho\frac{\partial (\omega U_j)}{\partial x_j}=\frac{\partial}{\partial x_j}\left[\left(\mu+\frac{\mu_t}{\sigma_{\omega,1}}\right)\frac{\partial \omega}{\partial x_j}\right]+\gamma_2\left(2\rho S_{ij}S_{ij}-\frac{2}{3}\rho\omega\frac{\partial U_i}{\partial x_j}\delta_{ij}\right)$$
$$-\beta_2\rho\omega^2+2\frac{\rho}{\sigma_{\omega,2}\omega}\frac{\partial k}{\partial x_k}\frac{\partial \omega}{\partial x_k}$$
$$-\rho\overline{u_i'u_j'}=\mu_t\left(\frac{\partial U_i}{\partial x_j}+\frac{\partial U_j}{\partial x_i}\right)-\frac{2}{3}\rho k\delta_{ij} \qquad (3)$$

3.1.2.2 Spalart-Allmaras Model

Equation (4) represents the second model being employed, the one equation Spalart-Allmaras turbulence model including the relationship that defines the Reynolds stress computations necessary to couple to Eqn. (2) [22]. This model represents a single transport equation for a kinematic eddy viscosity parameter $\tilde{\nu}$. Ω_{ij} represents the mean vorticity tensor.

$$\rho\frac{\partial\tilde{\nu}}{\partial t}+\rho\frac{\partial(\tilde{\nu}U_j)}{\partial x_j}=\frac{1}{\sigma_\nu}\frac{\partial}{\partial x_j}\left[(\mu+\rho\tilde{\nu})\frac{\partial\tilde{\nu}}{\partial x_j}+C_{b2}\rho\frac{\partial\tilde{\nu}}{\partial x_k}\frac{\partial\tilde{\nu}}{\partial x_k}\right]$$
$$+C_{b1}\rho\tilde{\nu}\tilde{\Omega}-C_{w1}\rho\left(\frac{\tilde{\nu}}{\kappa_{sa}y}\right)^2 f_w \qquad (4)$$
$$\tilde{\Omega}=\sqrt{2\Omega_{ij}\Omega_{ij}}+\frac{\tilde{\nu}}{(\kappa y)^2}f_{\nu 2}$$
$$-\rho\overline{u_i'u_j'}=\rho\tilde{\nu}f_{\nu 1}\left(\frac{\partial U_i}{\partial x_j}+\frac{\partial U_j}{\partial x_i}\right)$$

3.1.2.3 Turbulent Boundary Layer Wall Function

In addition, the presence of turbulent boundary layers requires an additional model which is given in Eqn. (5) [22] known as the law of the wall for turbulent boundary layers.

$$u^+=\frac{1}{\kappa}\ln(y^+)+B \qquad (5)$$

3.1.2.4 Turbulent Passive Scalar Transport Equation

Many methods of analyzing mixing are available and several will be used in this work. Among them is a direct simulation of the mixing of a passive scalar in the flow

field. This method requires an additional governing equation which is given by Eqn. (6) [22] and is referred to as a passive scalar turbulent transport equation.

$$\rho \frac{\partial \Phi}{\partial t} + \rho \frac{\partial (\Phi U_j)}{\partial x_j} = \frac{\partial}{\partial x_j}\left[\Gamma_\Phi \frac{\partial \Phi}{\partial x_j}\right] + \left[-\frac{\partial (\overline{u_j' \varphi'})}{\partial x_j}\right] + S\Phi \tag{6}$$

3.2 Computational Resources

The above equations were solved by means of two commercial general purpose CFD packages FLUENT [23] and Star-CCM+[24]. Even casual observation of the above models would no doubt recognize the presence of a significant number of empirical constants. Both software packages have default values selected for all empirical constants. In the current work these constants were unaltered in both programs.

The work described herein was completed with resources made available through the University's Center for High Performance Computing. In particular, simulations were completed on the Center's UNIX computing clusters: Uinta, Wasatch, and Sawtooth. Additional simulations were completed by means of the two Microway Whisperstations: Greenwood and Fremont in the HPC visualization lab.

CHAPTER 4

FULL LABSCALE RACEWAY SIMULATION EXPERIMENT DESCRIPTION AND OBJECTIVES

As the primary objective of this thesis was to investigate the hydrodynamics of algae raceways to better understand mixing and turbulence the first set of experiments to be carried out were simulations of an entire raceway whose dimensions were those of a raceway under consideration for experimental study.[1] This chapter is dedicated to the description of the rationale, methods, and objectives of this experiment.

4.1 Experimental Description

4.1.1 Raceway Geometry and Dimensions

In order to validate the impact that DWVGs have on algae raceways two simulations of a laboratory scale raceway having the dimensions shown in Table 4.1 (where the z dimension represents the width of a single channel) and a total volume of 1500 L were completed. The first simulation represents the control and as such has no DWVGs.

Table 4.1. Dimensions for Lab Scale Raceway

Dimension	Maximum Measurement (m)
X	4.16
Y	0.40
Z	0.46

[1] Following these simulations the proposed raceway was redesigned and thus a raceway with these exact dimensions was never built.

The second contains two DWVGs one at the center of each channel in the raceway Fig. 4.1 below shows this configuration. Note that the vertical plane in the back channel represents the location of the paddle wheel and that flow is in the clockwise direction when viewed from above, such that the tips of the delta wings represent the leading edges.

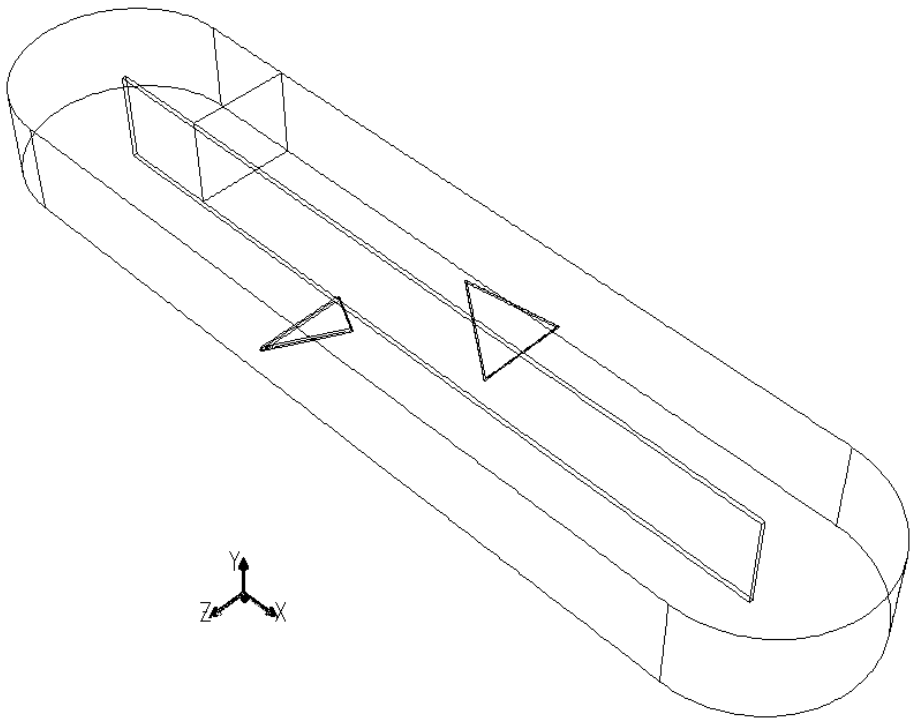

Figure 4.1. Layout for lab scale raceway

The configuration of the delta wings (i.e., size, placement, and angle of attack) selected for this experiment is largely arbitrary. CFD simulations were done to investigate the impact of angle of attack as well as the size of the delta wing relative to

the channel. These calculations lead to a rough estimation that if delta wings were found to have an impact it would be demonstrated by a pair at 35 ° angle of incidence, and a width 85% that of the channels themselves. The thickness of the delta wings is arbitrarily selected to be 4% of their width. Again, the placement at the center of the channels was arbitrary.

4.1.2 Software and Turbulence Model Selection

The governing equations were solved using the general purpose CFD solver FLUENT 13.0.0 [23].

Turbulence for the present experiment was modeled by means of the k-ω SST turbulence model. The rationale for this choice is that a primary objective of this experiment was the determination of environmental turbulence levels in the proposed raceway. As was stated in chapter 2, published research on algae sensitivity to turbulence always utilizes turbulent dissipation rate ε as the means of quantifying turbulence. Thus an acceptable turbulence model for the current work would have two basic qualifications: first that it be capable of modeling the physics of the flow, and second that it facilitate the determination of ε.

While any of the many variations on the classical k-ε two equation turbulence model would have met the second qualification they have documented [22] weaknesses that made them less than suitable from the perspective of the first qualification.

The k-ω SST model has been shown to have more robust performance for the types of flows studied in the current work [22] and has also served as the means of turbulence modeling for studies of a similar nature regarding flow over delta wings [25]. Thus it represented an acceptable turbulence model as long as determination of ε is

possible. Equation (7) [26] below gives the relationship between ε and ω that was used to accomplish this.

$$\varepsilon = \omega C_{\mu} k \tag{7}$$

where C_{μ} is a standard k-ε model constant and is assigned a value of 0.09.

4.1.3 Flow Parameters

The major parameter of interest in channel flow is the Reynolds number (Re), defined as

$$\mathrm{Re} = \frac{4R_h V}{\nu} \tag{8}$$

Here, R_h is the hydraulic radius, defined as the cross-sectional area divided by the wetted perimeter, V is the characteristic velocity defined in the present work as the mass average velocity in the raceway, and ν is the fluid kinematic viscosity. However, it is important to note that the addition of delta wings in a region of flow will impact the resistance felt by the power system responsible for driving the flow. This means that in order for a raceway to maintain the same characteristic velocity, and thus Re, the amount of power necessary must be higher than for a raceway with no delta wings. In an effort to ensure that the results were economically equivalent, both configurations were run at approximately the same power input. This has the impact of slightly reducing the Re in the raceway with the delta wings. Thus the primary flow parameter of interest is actually the power requirement into the paddle wheel. The power required to drive the flow around the raceway is determined from the energy equation to be:

$$P_r = Q\Delta p \tag{9}$$

where, P_r is the power required in J/s for an ideal paddle wheel that suffers no inefficiencies, Q is the volumetric flow rate in the channel in m^3s^{-1}, and Δp is the pressure loss in the channel in Pa.

4.1.4 Numerical Method

All of the governing equations in the model employed the second order upwind scheme to interpolate values to the cell faces; a second order temporal discretization was also used. The top of the raceway was modeled using a zero shear stress rigid lid approximation for the free surface. This was done to avoid the necessity of modeling two different phases. In the work of Spall et al. [27] it was shown that the two phase modeling can be an unnecessary complication that offers little additional accuracy, this was assumed to be the case in the present work. All other solid surfaces were assigned the traditional no-slip boundary condition. Standard wall functions were used with this model to handle the near wall region.

There were two methods considered for modeling the paddle wheel driving the flow around the raceways: a dynamic mesh model of an actual paddle wheel, and a simplified approach using fan-type boundary condition. The dynamic mesh model is a complicated procedure that would allow for the exact geometry of the paddlewheel to be meshed, and to move through the otherwise stationary mesh of the raceway. While this procedure would add more accuracy, it is computationally expensive and technically difficult. Consequently, the second method was chosen. Though this approach will not correctly predict the impact of the paddlewheel, especially in the area it occupies, it is

assumed that the impact to the overall accuracy of the model is small. A fan-type boundary condition represented by a discontinuity in the pressure was specified at the location of the paddle wheel (see Fig. 4.1). This greatly facilitated the determination of the power requirements since the only remaining variable is Q. Through an iterative process, it was determined that a value for Δp of 400 Pa in the raceway with no delta wings was roughly equivalent, in terms of power requirements, to a Δp of 424 Pa in the raceway with the delta wings placed as shown in Fig. 4.1.

The initial step in the solution procedure was to allow the simulation to evolve until a quasi-steady-state flow developed. This refers to a state where the volumetric flow rate is changing minimally with time, which is only a result of the unsteady influences of vortex generation over the different edges in the domain. It was noted that about 18 seconds was sufficient to ensure that both configurations had reached this condition. Around 10–15 iterations per time step were required to decrease the residuals to order 10^{-4}. At this stage the governing equations of fluid motion (2, 3, and 5) were disabled and the velocity and turbulence fields frozen. The flow fields of both simulations were then analyzed and compared in order to determine the impact of DWVGs on raceway vertical mixing and turbulence.

4.1.5 Mesh Dependency and Error Estimation

A concern of any work that involves simulation is that of quantification of potential errors in the solution. When working with CFD a source of major concern is the impact, if any, that the mesh used to discretize the domain has on the quality of the solution. For this reason best practices for establishing mesh independency of results as well as error estimation have been developed.

For the current work a series of three subsequently refined meshes was used to complete the first stage of the simulation for both the control and experimental cases. A value of significant interest to the results of this study was monitored for all of these cases and the results of each mesh for both cases were compared to each other in order to determine the impact that the mesh had on the parameter. For the current work the parameter selected was power requirement as calculated by Eqn. (9).

In addition a more formal approach of estimating the error was employed, that of Richardson extrapolation. This method uses the results of the three meshes and computes an estimation of the uncertainty due to discretization. The details of this method as well as additional information on the motivation and necessity of error analysis in CFD can be found in the report by Celik et al. [28].

4.1.6 Vertical Mixing

Vertical mixing was investigated qualitatively by means of velocity vector plots located at key locations in the raceway relative to the location of the DWVGs. In particular these were used to investigate the presence of any structures in the flow that would be expected to have an impact on the levels of vertical mixing. The maximum and minimum values of the vertical component of velocity in these plots were also compared in order to determine the intensity of motion in the vertical plane at these locations and compare them between configurations.

The main tool used to quantify the effectiveness of vertical mixing in the entire raceway was mixing time. In order to define this mixing time a concentration profile for a passive scalar consisting of a scalar concentration of zero in the lower half of the raceway and unity in the upper half was defined after the velocity and turbulence fields

were frozen. Subsequently the passive scalar transport equation was solved and concentration as a function of time was monitored at 20 randomly selected vertex points in the domain. In addition, the area weighted average scalar concentration at two horizontal planes in the flow (one 10% the other 90% of the total depth from the raceway floor) were also be monitored as a function of time. The mixing time is defined as the time necessary for the concentration difference, as a percent of initial concentration difference, to fall below some tolerance. The concentration difference percentage is defined as:

$$\Delta\Phi(t) = ABS\left(\frac{\Phi(t) - \overline{\Phi}}{\Delta\Phi_0}\right) * 100 \tag{10}$$

where $\Phi(t)$ is the scalar concentration as a function of time, $\overline{\Phi}$ is the total raceway mass averaged concentration, and $\Delta\Phi_0$ is the initial difference between the concentration at the point or plane of interest and the total mass average concentration. Because of the nature of the initial concentration profile, the mixing time measured in this manner is essentially a quantification of the vertical mixing present in the raceway. A value of five percent was selected as the tolerance.

The time necessary for each of the 20 vertex points and, separately for the two planes, to fall below the tolerance, was averaged in order to come up with two mixing time estimations. It should be noted that mixing time calculations performed in the manner described above are highly sensitive to the location of the concentration measurements; this is the reason for developing two separate methods.

4.2 Experimental Objectives

The primary objective of this experiment was to investigate the impact of DWVGs on a lab scale raceway. In particular a comparison of the vertical mixing present in a raceway with and without DWVG's was desired. In addition this experiment served the purpose of studying the levels of turbulence present in algae raceways, both for comparison between the control and experimental raceway as well as comparison with published data on algae sensitivity to turbulence.

CHAPTER 5

FULL LABSCALE RACEWAY SIMULATION EXPERIMENT

RESULTS AND DISSCUSSION

The results of the full lab scale raceway simulation are presented and discussed in this chapter. Power requirement and mesh dependency results are reported on together as the power requirement served as the parameter of interest for the determination of the fine grid convergence index (GCI). Velocity vector plots and mixing time results are used to analyze the levels of vertical mixing in the present raceway. In addition the turbulence levels are reported on and analyzed, both a comparison between configurations as well as to published values in literature relating to algae growth are given.

5.1 Mesh Dependency and Power Requirement Results

Table 5.1 below details the characteristics of the three meshes used for the control simulation as well as the three used for the DWVG configuration in both number of cells and characteristic cell size as it is determined in [28]. Additionally vector plots of the flow field were compared between the three meshes as a qualitative measure of the mesh dependency of the solution, these results are given in the section on velocity vectors.

Results for the power requirements (in units of Watts) of each of the grids at time equal to 18.5 seconds are given in Table 5.2. It is clear from the data that as the quasi-steady-state conditions described in section 4.1.4 are achieved the solutions are nearly grid independent in terms of power consumption, as the maximum difference seen between grids is 1.7% in the case without DWVGs, and 0.5% in the case with DWVGs.

Table 5.1. Number of Cells and Cell Characteristic Size for Each Raceway Configuration

No Delta Wings			
	Grid 1	**Grid 2**	**Grid 3**
Number of Cells	345,664	1,059,459	2,541,279
Characteristic size (m)	$1.602\ 10^{-2}$	$1.103\ 10^{-2}$	$8.238\ 10^{-3}$
2 Delta Wings			
	Grid 1	**Grid 2**	**Grid 3**
Number of cells	351,835	1,037,164	2,012,139
Characteristic size (m)	0.015917	0.011101	0.008901

In addition the fine grid convergence index produced from Richardson extrapolation shows that the solution is well converged with minimal error. Also, it is apparent that the power requirements both with and without delta wings are essentially the same, making any vertical mixing comparisons economically relevant.

Table 5.2. Power Requirement (W) at t=18 sec, Max Error and GCI for Each Grid

Configuration	**Grid 1**	**Grid 2**	**Grid 3**	**Max Error (%)**	**GCI_{fine}[21]**
0 delta wings	26.91	27.16	27.37	1.7	1.085 E-1
2 delta wings	27.26	27.23	27.16	0.5	2.942 E-4

Representative meshes for Grid 3 used in the simulation of the DWVG configuration are given below in Figs. 5.1 and 5.2. Figure 5.1 shows a cross section view of the polyhedral mesh surrounding the DWVG at a z location of 0.22 m. Figure 5.2 shows the surface mesh on the delta wings vortex generator. Both of these meshes were used in conjunction with wall functions so as to not resolve the turbulent boundary layer.

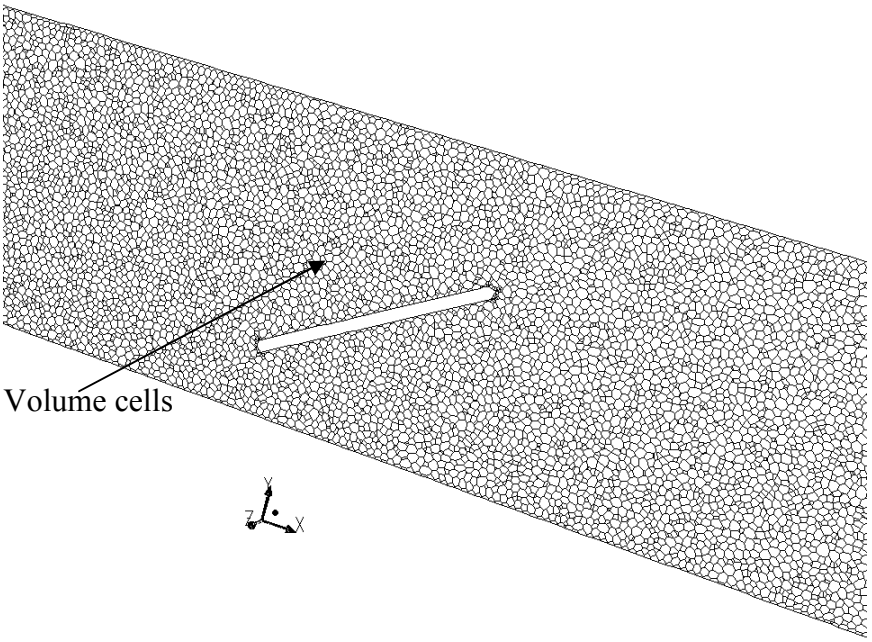

Figure 5.1. Representative mesh along x=0.22 m plane for grid 3

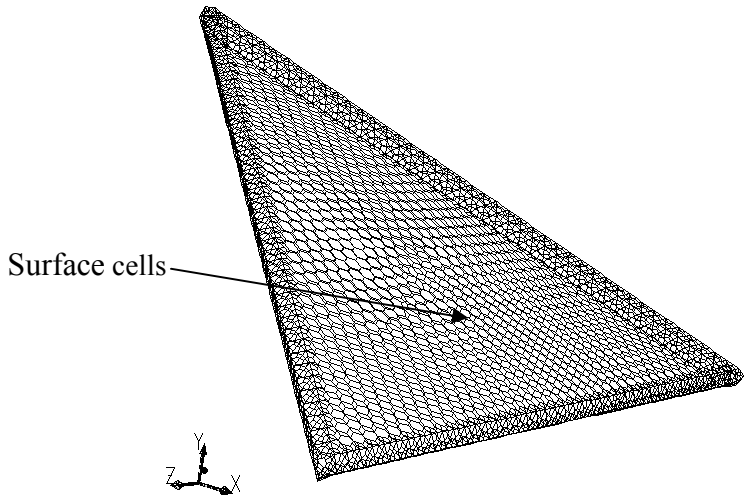

Figure 5.2. Representative DWVG surface mesh from grid 3

5.2 Velocity Profiles

Images of the velocity profiles were used both to assess grid independence as well as to compare the vertical mixing in key areas in the raceway. Figures 5.3a, b, and c show velocity vectors for the zero delta wing case at the plane x = 2.5 meters for all three grids. Only the portion of the plane that rests in the same channel as the paddle wheel was examined. Figures 5.4a, b, and c show the same profiles for the case with delta wings. Of the three profiles that correspond to the zero delta wing raceway, the two that represent the finer meshes are in excellent general agreement. The coarsest mesh, however, has at least one specific structure at the bottom of the channel that is not found in the others. Consequently, the two finer grids will be primarily considered in the section that investigates mixing time. In the case with delta wings there is excellent agreement between all three grids.

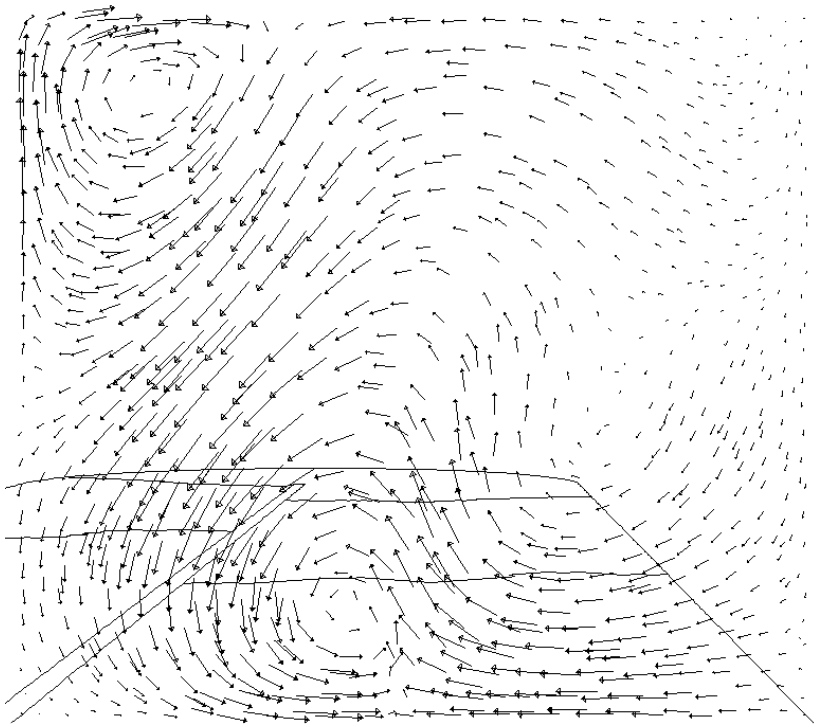

Figure 5.3-a. Velocity vectors in plane x=2.5 METERS for the grid 1 solution of the zero delta wing raceway

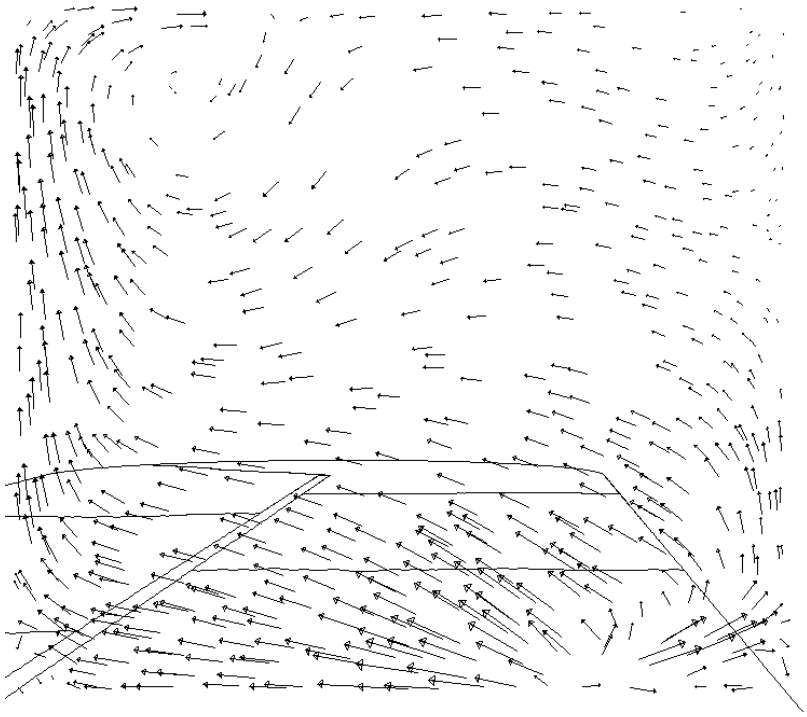

Figure 5.3-b. Velocity vectors in plane x=2.5 METERS for the grid 2 solution of the zero delta wing raceway

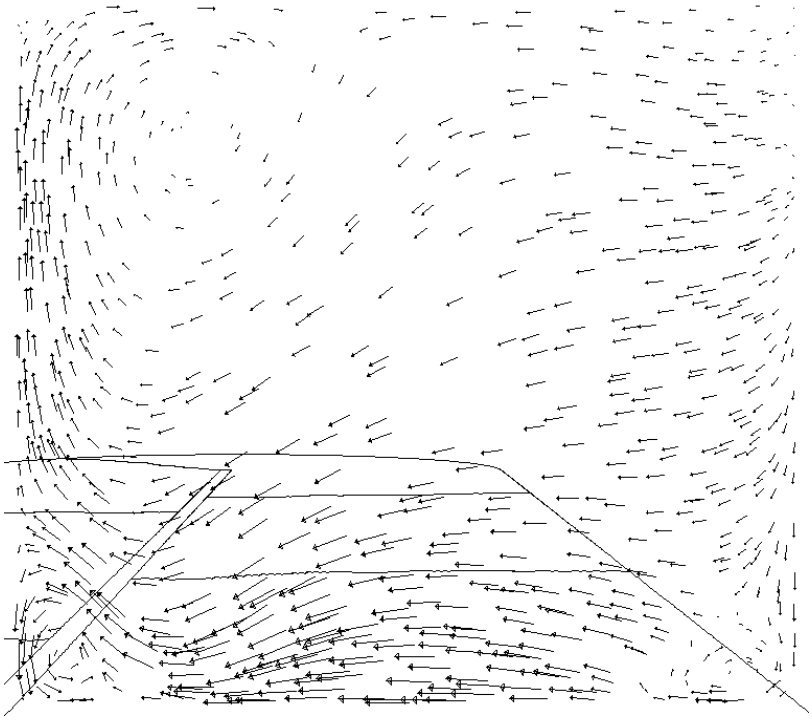

Figure 5.3-c. Velocity vectors in plane x=2.5 for the grid 3 solution of the zero delta wing raceway

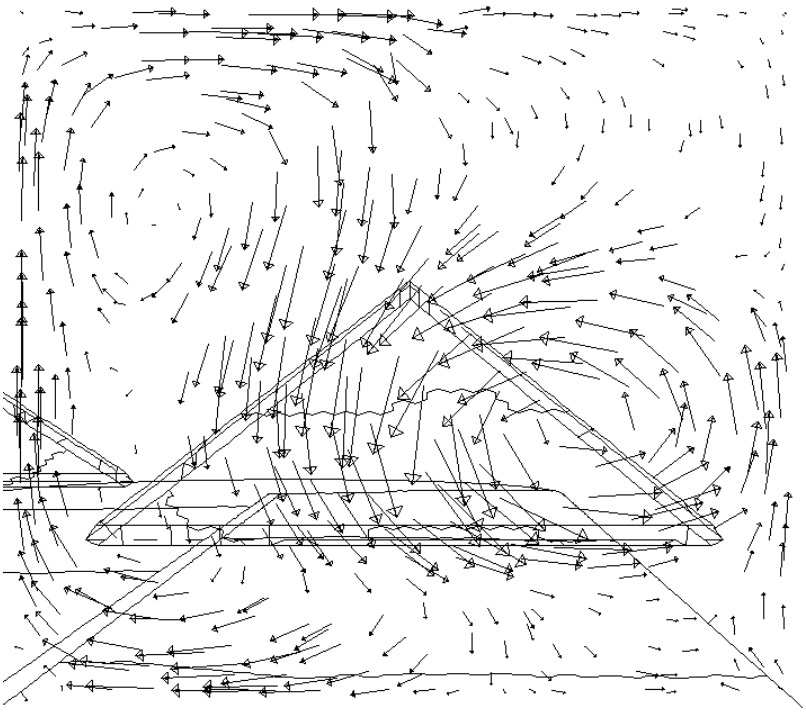

Figure 5.4-a. Velocity vectors in plane x=2.5 for the grid 1 solution of the delta wing raceway

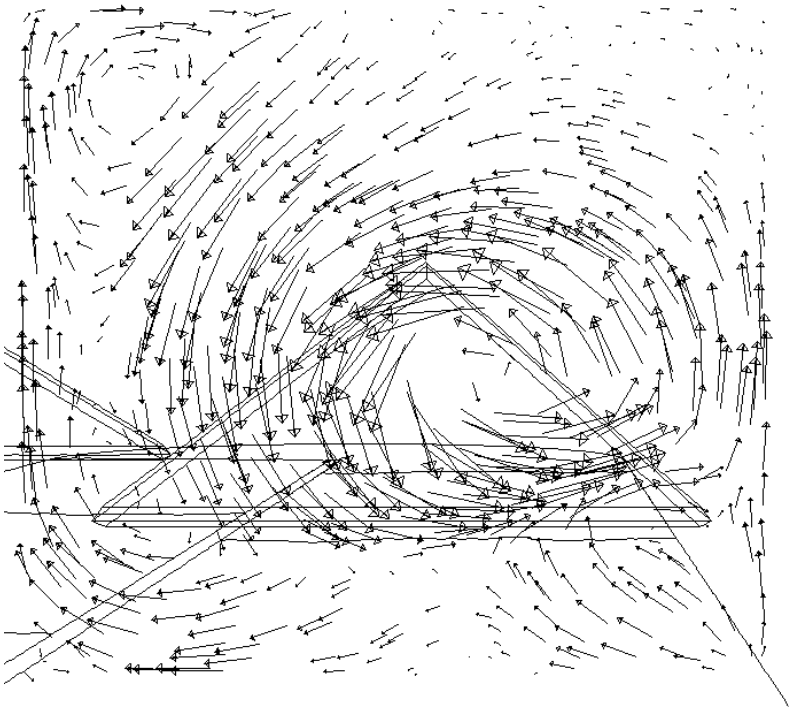

Figure 5.4-b. Velocity vectors in plane x=2.5 for the grid 2 solution of the delta wing raceway

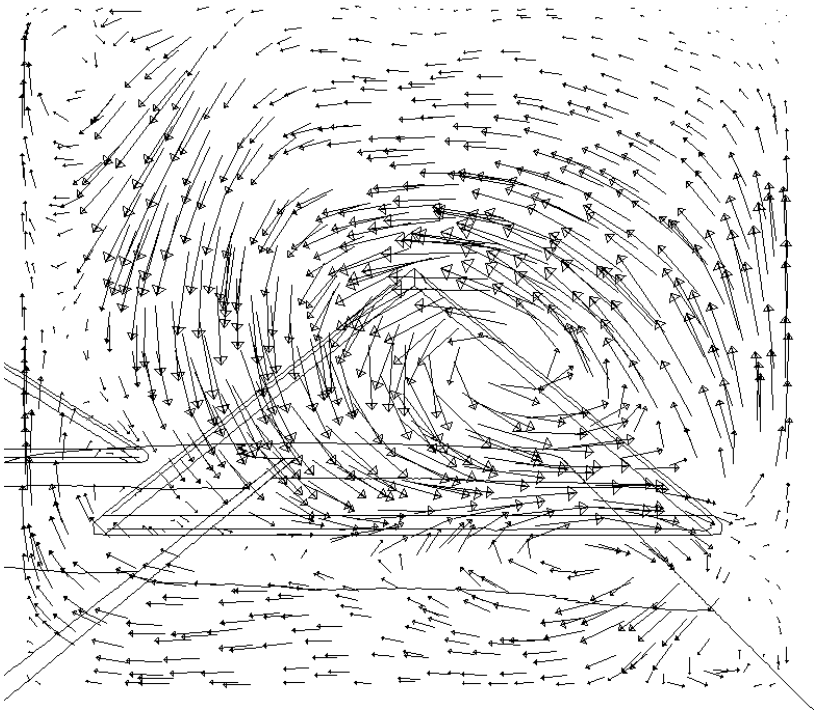

Figure 5.4-c. Velocity vectors in plane x=2.5 for the grid 3 solution of the delta wing raceway

These figures were also used to investigate the impact that the delta wings had on the vertical motion in their immediate vicinity. In comparing Figs. 5.3-a through c to Figs. 5.4-a through c it is clear that the presence of the delta wings induces significant motion in the vertical plane. This finding suggests that the addition of the delta wings would enhance vertical mixing in algae raceways. In addition to these structures, the intensity of vertical motion was also increased. Table 5.3 shows the maximum and minimum vertical velocities for the profiles in Figs. 5.3-c and 5.4-c. It is clear that the magnitude of the velocity in both the positive and negative y directions was increased significantly with the addition of delta wings. This finding further supports the idea that delta wings would in fact generate more frequent opportunities for algae to gather light energy near the surface of the raceway.

Table 5.3. Max and Min Vertical Velocities in the x=2.5 m Plane

	0 Delta Wings	2 Delta Wings	% Magnitude Increase
Min y velocity (m/s)	-0.29	-0.42	44.8
Max y velocity (m/s)	0.33	0.67	103.0

5.3 Turbulence Results

Values of ε were compared between the two raceways. Specifically, the total raceway mass averaged value, and the area weighted average value for the x=2.5 plane (shown in Figs. 5.4 and 5.5) were compared and the results are shown in Tab. 5.4 below for the finest grids. The results indicate that turbulence as measured by either method is significantly increased by the addition of DWVGs. This is particularly true in the region near the DWVGs themselves.

Table 5.4. Comparison of Turbulent Dissipation Rate between Two Raceway Configurations. The mass average results are taken over the entire raceway, while the area average results are reported for the x=2.5 m plane.

Method	0 DW	2 DW	% Increase
Mass avg. ε (m^2/s^3)	$1.287\ 10^{-2}$	$1.425\ 10^{-2}$	10.7
Area avg. ε (m^2/s^3)	$1.746\ 10^{-2}$	$2.187\ 10^{-2}$	25.2

It should also be noted that the levels of ε in both cases is almost an order of magnitude larger than the highest values of ε in the literature [4-7]. Even without delta wings the turbulent dissipation rate that is characteristic to raceway flow is significantly higher than the levels typically experienced by algae in the ocean or in lakes and ponds.

These results have serious implications for researchers working to create optimum ABD production systems. Certain species of algae have been shown to dramatically increase or decrease their growth as a result of environmental turbulence. Given the knowledge that raceway turbulence has the potential to be significantly higher than the

threshold normally considered high in published literature, and the fact that addition of DWVGs has the potential to increase the levels even further, raceways are potentially a very toxic environment to some species of algae. This will effectively require that in the selection of algae strain, consideration must be given to the organism's robustness in turbulent environments.

5.4 Vertical Mixing

Table 5.5 below compares the mixing times between the two different raceways for the fine grids. It appears that the mixing time is not significantly impacted by the addition of delta wings. Though the 20 point method shows a slight decrease in mixing time, the two plane method shows a slight increase. In each case however there is not a significant change in the mixing time. The two delta wings thus seem to have a negligible impact on the overall vertical mixing in a raceway. These results seem to indicate that the presence of two delta wings in the configuration tested in the present work were not a significant enough influence on a raceway of the dimensions considered.

Table 5.5. Mixing Time Comparison between Raceway with and without Delta Wings Using both the Point and Plane Methods

	0 DW	**2 DW**
20 point method (s)	18.8	17.5
2 plane method (s)	9.2	10.4

Figures 5.5 and 5.6 show $\Delta\Phi$ as a function of time for each of the points and the planes used in the mixing time calculations for both raceways. It is clear from these two figures that the vertical motion in the raceway is impacted by the delta wings. The two figures show different profiles of $\Delta\Phi$ over time, however, the end result seems to be an

average mixing time that is roughly the same. This is evident because the amount of time necessary for the majority of the points in the figure to fall below the 5% tolerance is very near 45 seconds in both figures. These figures in conjunction with the mixing time calculations illustrate that neither raceway is experiencing a significant increase in vertical mixing compared to the other.

Though the values are not reported on here, a sensitivity study on the tolerance was conducted. The results indicated that the conclusions based on mixing time are not impacted by the tolerance, as any value selected led to the same conclusions for both raceway configurations.

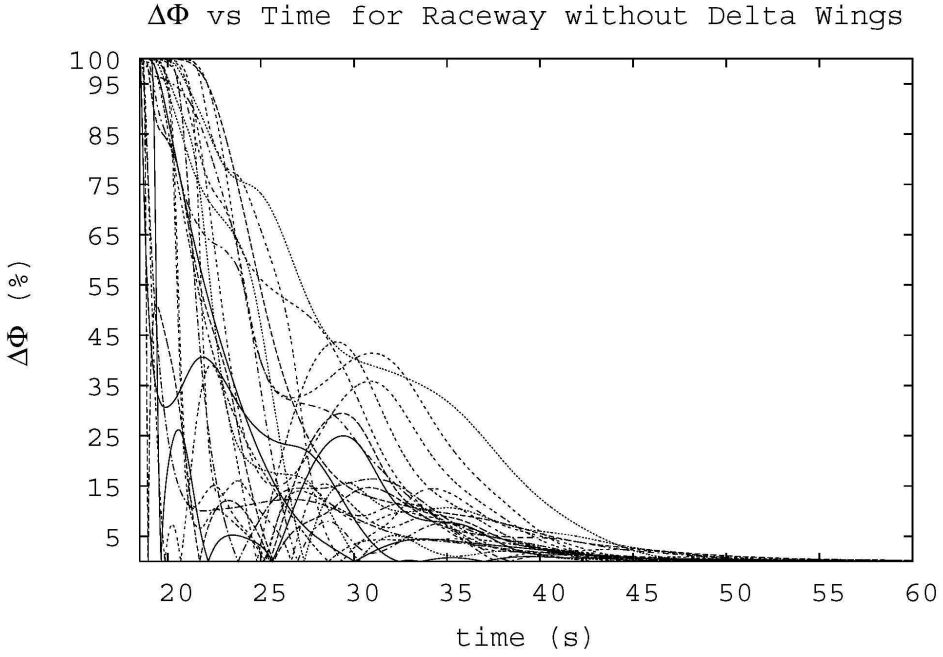

Figure 5.5. Scalar concentration difference from mass averaged value as a percent for all points and planes monitored for mixing time calculations for the raceway without delta wings. Each line represents a single point or plane at which concentration was monitored.

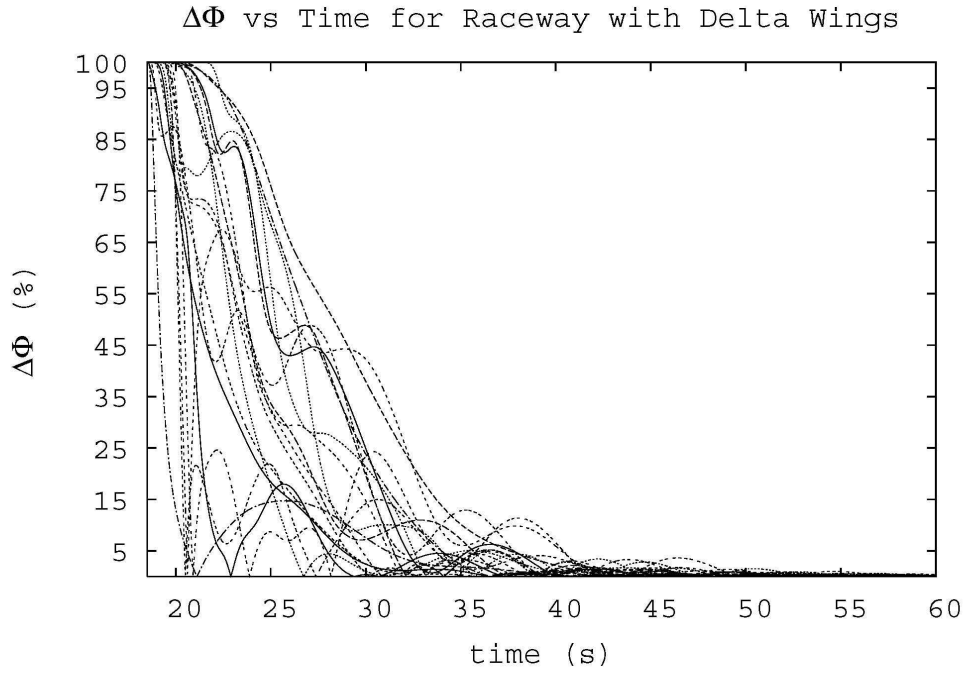

Figure 5.6. Scalar concentration difference from mass averaged value as a percent for all points and planes monitored for mixing time calculations for the raceway with delta wings. Each line represents a single point or plane at which concentration was monitored**.**

5.5 Discussion

The simulations completed on a potential lab scale algae biofuel raceway with the addition of DWVGs allowed for a thorough investigation of their impact on power requirement, turbulence, and vertical mixing. The simulations were carried out in manner with appropriate verification measures such that the results can be considered accurate.

Of significant importance to the future applications of the current work is the impact that the proposed alterations in the raceway might have on the power system requirements. In an effort to establish the results of the current work as economically viable the flow conditions of the two raceways was modified such that the power required

to drive the flow is the same or very close. This was accomplished by decreasing the velocity in the raceway with the DWVGs.

It was anticipated that with the increases in vertical mixing associated with these devices, even at lower velocities, superior levels of vertical mixing would be achieved at no additional power costs. The results however give contradictory information. Plots of the velocity vectors near the DWVGs showed a significant increase in motion in the vertical plane. The mixing time, however, yielded much less conclusive results. The DWVG configuration had a mixing time that showed no significant difference from that of the control configuration. Thus it seems that DWVGs as least in the configuration investigated were incapable of significantly impacting the vertical mixing of the raceway was a whole.

When these results are considered in sum they give indications that additional vortex generation devices are required in order to have a significant impact on the vertical mixing in a raceway as a whole. Given this possibility the questions of pressing interest are regarding the impact that spacing of DWVGs has on the intensity of vertical mixing, as well as the power requirements necessary to drive the flow. In addition a more formal investigation of the time impact of angle of attack on these two parameters is also of interest. These questions form the basis for the remaining research presented in this thesis and are covered in the following chapters.

CHAPTER 6

SPACING AND ANGLE OF ATTACK EXPERIMENT

DESCRIPTION AND OBJECTIVES

Previous work having suggested the potential of DWVGs to increase raceway vertical mixing, it became necessary to further investigate the hydrodynamics associated with these flow obstructions. In particular, it is clear that for meaningful results a series of DWVGs would be necessary. The impact that such a configuration could have on the power requirements needed to be studied. In addition it was apparent that for optimal design a better understanding of the impact of angle of attack on vertical mixing and power requirements is necessary. This chapter outlines the methods and rationale behind the set of experiments employed to further understand these relationships.

6.1 Experimental Description

6.1.1 Geometry Dimensions and Configuration

As the objective of this experiment is to understand the impact that DWVG spacing has on the objective of generating vertical mixing, a method of simulating a series of vortex generators was required. Though this is possible by means of brute force simulations of large raceways with several DWVGs placed in series it is by no means practical as the scope and size of such simulations would become daunting and almost certainly limit the spacings investigated to a very small number. Fortunately a more elegant method exists for obtaining the desired information.

It is first noted that the information necessary does not require the simulation of entire raceways. The impact of the spacings relative to each other will be just as apparent

in simulations of a straight segment of channel, akin to those found on either side of a raceway. This alone has the potential to significantly reduce the size and complexity of the simulations.

Additional simplifications were also available through the selection of the appropriate boundary conditions. The field of CFD requires the numerical modeling of physical boundary conditions to be applied to the governing equations described in Chapter 3. Fortunately among the many boundary conditions that have been developed is a periodic condition that takes the conditions present at one boundary and duplicates them at another.

This tool proved very useful in a study of the impact of spacing. The inlet and outlet faces of a channel were designated as a pair of boundaries making up a periodic condition. In this way the flow conditions present at the outlet of the channel were duplicated at the inlet allowing the resulting simulation to represent the flow developed in a straight channel with a series of many DWVGs all spaced a distance equal to the length of the channel segment one from another. Conditions at these boundaries are constrained by a constant mass flow rate which of 40 kg sec^{-1} which corresponds to an average velocity magnitude of 0.3 m sec^{-1}. This value was chosen as it represents a typical average velocity in raceways used for algae cultivation.

A series of geometries, identical to one another with the single exception of the segment length were studied. Figure 6.1 below contains a representation of one such geometry. The angle of attack of the DWVGs was set to 40 degrees for all these cases. The dimensions of the width and the depth of these channel segments was made to match those of the experimental raceway located in SANT 202A. As this raceway is capable of

studying multiple depths it was necessary to identify which of its depths would be used for these studies. The deepest configuration for which the SANT raceway was designed was selected (12 in). The justification for this is that the eventual goals of this research are to maximize the depths at which effective algae growth can take place. The width of the delta wings mimicked that of experiment one, they were 85% the total width of the channel. The thickness was again set to 4% of the delta wing width. The investigated channel lengths were measured in numbers of delta wing widths (DWWs). Seven were selected for study starting at 1.5 DWWs and incrementing by half a DWW, the maximum spacing studied being 4.5 DWWs.

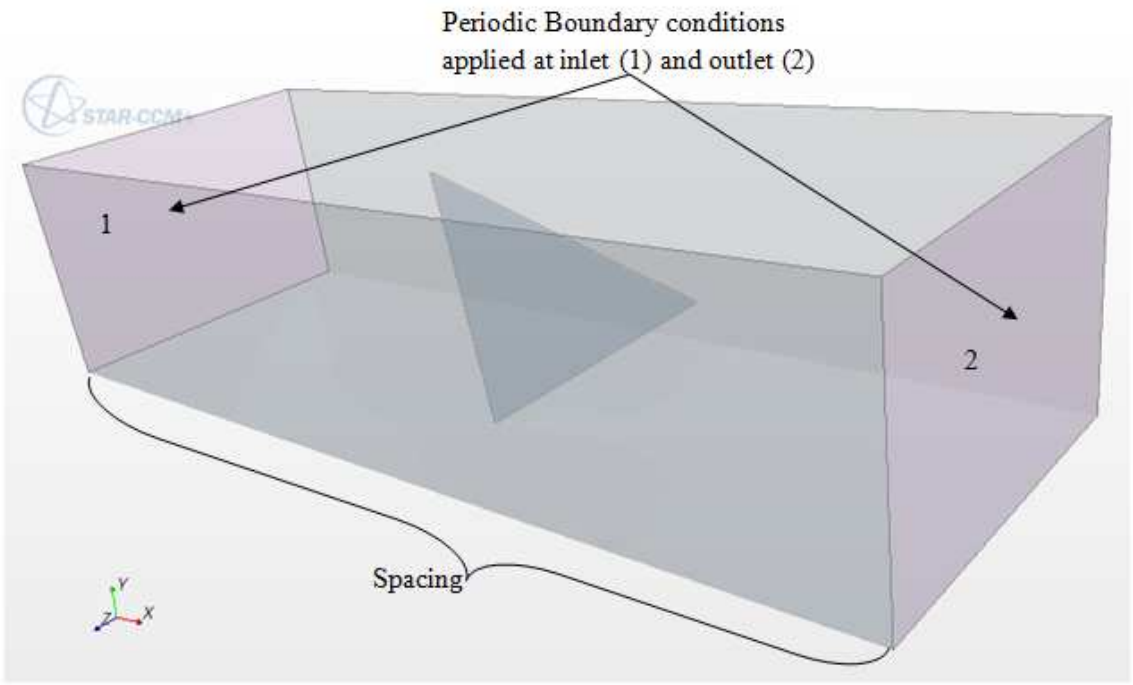

Figure 6.1. Layout of representative channel segments used in spacing study

This same configuration also served as the model for the experiments aimed at understanding the impact the DWVG angle of attack has on vertical mixing and power requirement. A single spacing of 2 DWWs was employed for the angle of attack study,

this selection was in and of itself rather arbitrary from the stand point of mixing or power requirement, the rationale simply being to study cases that would have a smaller number of cells.

6.1.2 Software and Turbulence Model Selection

The general purpose CFD package Star-CCM+ [24] was used for to complete all of the simulations for this set of experiments.

The current work had less stringent requirements of an appropriate turbulence model. The results reported on in chapter 5 concerning turbulence dissipation rates as an indication of environmental turbulence were sufficient to make comparison to published research. Consequently ε values were not required for the current experiments, and the only requirement of a turbulence model be that it be capable of sufficiently handling the physics of the flow. Given the distinct similarities between the present work and many aerospace flow simulations the Spallart-Almaras (SA) model defined in chapter 3 was an appropriate selection. While the k-ω SST model employed previously would in theory also be acceptable, the SA model exhibited a superior capacity for reduction in the normalized residuals of the governing equations, this served as the justification for its selection.

Given the large scale of the complete raceway simulations it was deemed best to rely heavily on the use of turbulent wall functions. As the geometry of the current simulations was more constrained and the details of comparison in vertical mixing and power requirement between configurations of similar sizes a more accurate handling of the turbulent boundary layer was required. For this reason it was determined to pursue

complete resolution of the turbulent boundary layer. In order to accomplish this each configuration required a wall y+ of ~ 1 on all the no-slip walls.

6.1.3 Flow Parameters

The objectives of the current study are in many ways similar to those of the work described in chapters 4 and 5. As such, many of the same parameters are used in the current experiments. In particular, as the impact of various DWVG configurations on system power is being studied, a measurement of the system power is necessary. This is largely achieved in the same manner as for experiment 1. Equation (9) again serves as the appropriate relationship for the determinations of power requirement. The use of periodic boundary conditions as opposed to the fan condition employed in experiment one alters slightly the determination of the pressure drop Δp. Equation (11) below gives the equation used in the determination of this value. Where the bar represents an area weighted averaging. The volumetric flow rate in this case is fixed by the periodic boundary condition which enforces the mass flow rate (set at 40 kg sec^{-1}). This value divided by the density gives the volumetric flow rate.

$$\Delta p = \overline{p}_{outlet} - \overline{p}_{inlet} \tag{11}$$

Additional manipulation of this term is required for comparison between spacings. Lengthening the section of channel will result in additional losses due to the additional surface area of no-slip walls. A better method of comparison for the current experiment is to take the mass specific power requirement where the power obtained

from Eqn. (9) is divided by the mass of water in the channel segment. This allows for direct comparison between configurations of different spacings.

Vertical mixing is the other parameter of interest in the current work. The method of determining a characteristic mixing time described in chapter 4 is complicated and selection of appropriate random points is difficult as comparisons are being made between configurations of differing geometries. These observations necessitated the selection of an alternate means of determining the vertical mixing in for the current work. An improved method that is effective for comparison between channels of different lengths is to define a parameter vertical mixing intensity. The relationship for this term is given below in Eqn. (12).

$$M_I = \frac{\frac{1}{V}\int ABS(U_2)dV}{\overline{V}} \tag{12}$$

This represents a volume average of the absolute value of the vertical component of the mean velocity. This value is normalized by the averaged velocity in the channel segment (0.3 m/s). The absolute value is necessary as a result of the constraint from continuity that the positive and negative components of vertical velocity will cancel over the entire volume.

6.1.4 Numerical Method

All of the governing equations in the model employed the second order upwind scheme to interpolate values to the cell faces. Though nothing in this experiment required unsteady simulation it was discovered that to obtain sufficient reduction in the

normalized residuals an unsteady solver was required. As this was the case a second order temporal discretization was also used. The top of the raceway was again modeled using a zero shear stress rigid lid approximation for the free surface. All other solid walls were treated with the no-slip boundary condition.

In order to speed up the time to solution a steady state approximate solution was first obtained. The flow parameters of interest to this work were monitored during this time, once these values were no longer changing significantly with each iteration, and the normalized residuals had ceased to decrease the solver was changed to unsteady. This generally required about of 1100 to 1300 iterations. Subsequent unsteady simulation was successful in reducing the residuals to acceptable levels, in most instances 10^{-4}, however for some of the shorter spacings investigated the continuity residual was unable to be reduced below 10^{-3}. It was noted that the values of the flow parameters did not change in any significant way following the switch to an unsteady solver.

6.1.5 Mesh Dependency and Error Estimation

Error estimation was handled similarly to the whole raceway simulations. The effect that the mesh had on the solution was investigated by a grid refinement study. The results of which were also used to define the fine grid convergence index. This study was not completed for each of the cases investigated, as the similarities were such that a single study on a single spacing would be sufficient to determine the impact that the mesh had on all spacings. For this reason the 3.5 DWWs spacing was selected to complete this study, this selection was largely arbitrary, however, it seemed prudent to select a spacing in the middle range of those being investigated. Both the vertical mixing intensity as well as the mass specific power requirement were used for fine grid convergence index

determination. Additionally as was stated in the previous section normalized residuals were reduced to at least 10^{-3} in order to ensure accurate solutions.

6.2 Experimental Objectives

The current research builds off of the results obtained by the raceway simulations. Having provisionally identified the potential for DWVGs to increase vertical mixing in algae cultivation raceways, it was necessary to better characterize some of the design parameters that are available for manipulation. The previous research made clear that in order to be successful a series of DWVGs would be required and thus a design parameter of critical interest is the spacing between vortex generators. In addition it is expected that the angle of attack would have a significant impact on the mixing intensity. The work described in the current chapter has as objectives to show the relationship between these two parameters and the levels of vertical mixing in channel segments. In addition it is desirable to understand the impact that both of these parameters have on the power requirement of the flow that develops.

These objectives are met primarily by plots of the relevant flow parameters vs. each of the design parameters (spacing and angle of attack). In addition, it is desirable to investigate these results for optimum configurations. This is done by plotting the vertical mixing intensity divided by the mass specific power requirement vs. the spacing and angle of attack. These plots are then used to determine configurations with the most favorable mixing to power requirement ratios.

6.3 Explanation for Procedural Variance between Experiments

It will be noted from the experimental methods presented in chapters 4 and 6 that substantial differences exist, particularly in the definition of vertical mixing. The explanation for this lies in the fact that significant improvements in understanding vertical mixing and the best method for quantifying it were made during the research described in Chapter 4 and reported on in Chapter 5. These improvements in methodology were subsequently developed during the completion of the simulations described in section 6.1.3. Ideally this method would have been retroactively applied to the results obtained for the earlier raceway experiments. However, by the time this secondary method had been developed the Lab had decided to move from FLUENT to Star-CCM+. Unfortunately simulation files generated in FLUENT are not compatible with Star-CCM+ and thus the results were not able to be analyzed via the second method.

CHAPTER 7

SPACING AND ANGLE OF ATTACK EXPERIMENT

RESULTS AND DISSCUSSION

Computational experimentation of the impact of vortex generator spacing and angle of attack were completed. This chapter is dedicated to the presentation of the results of these experiments as well as discussion of the significant features of these results. Mesh dependency as well as error estimation are treated first. Velocity vectors as well as streamline representations are given in order to qualitatively describe the flow throughout the entire domain. Subsequently, vertical mixing intensity and power requirement results are given for both sets of experiments. These results are discussed and their implications for optimal raceway design are presented.

7.1 Mesh Dependency and Error Results

Table 7.1 below gives the mesh characteristics for each of the three meshes (Grids 1, 2, and 3) used to complete this portion of the study, including the number of cells and the characteristic cell size as determined by the method given by [28]. Results from these three meshes were compared qualitatively by means of velocity vector plots as well as quantitatively by means of comparison of critical flow parameters as wells as Richardson extrapolation.

Table 7.1. Number of Cells and Characteristic Cell Size for Experiment Two Mesh Dependency Study

	Gird 1	**Grid 2**	**Grid 3**
Number of Cells	1,966,896	2,901,396	5,071,983
Characteristic Cell Size	$4.396\ 10^{-3}$	$3.862\ 10^{-3}$	$3.206\ 10^{-3}$

Results for the vertical mixing intensity and mass specific power requirement for each of the three grids are given in Tab. 7.2. Again it is seen from the results that the solutions on all three grids are in excellent agreement. The maximum error for the vertical mixing intensity is 3.2 %, and 2.1 % for the mass specific power requirement. The convergence index was acceptably low in both cases. These results in conjunction with sufficient residual reduction indicate that confidence in the simulations is justified.

Table 7.2. Max Percent Error and Fine Grid Convergence Index for Mixing and Power Requirement Results of Spacing Experiment

	Grid 1	**Grid 2**	**Grid 3**	**Max Error (%)**	**GCI_{fine}^{21}**
M_I	0.3932	0.3952	0.3828	3.243	$1.229\ 10^{-2}$
P_s (mW/kg)	5.6300	5.5120	5.5222	2.141	$7.749\ 10^{-5}$

Representative surface meshes and volume meshes are given below. Figure 7.1 is the DWVG surface mesh for grid 3 used in the determination of the GCI. Figure 7.2 shows a zoomed in view of the same surface mesh in the region of one of the DWCG corners. This image shows clearly the additional mesh refinement applied to this region as well as all the edges and corners. Figure 7.3 shows a representation of the volume mesh in the region surrounding the DWVG. In particular the prism boundary layer mesh that was applied in order to resolve the turbulent boundary layer is shown. The average value of y+ on all no-slip surfaces for this simulation was 1.027 which is ideal for boundary layer resolution. Additionally Fig. 7.3 shows that refinement in the volume mesh was carried out in the regions near the DWVG edges and corners. This was done in order to better resolve the large velocity gradients present in these regions. Though only meshes for the 3.5 DWW case are shown they are characteristic of all the cases as the

fine mesh used in grid three served as the blueprint in all others. Additionally the resulting y+ reported on above is representative of the results for all the cases run.

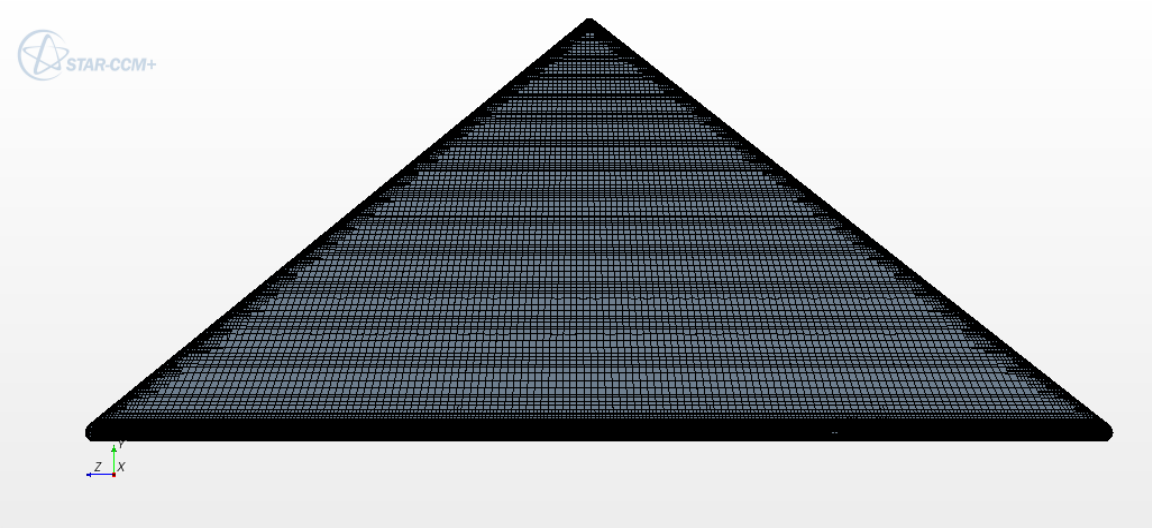

Figure 7.1. Representative DWVG surface mesh used in grid 3

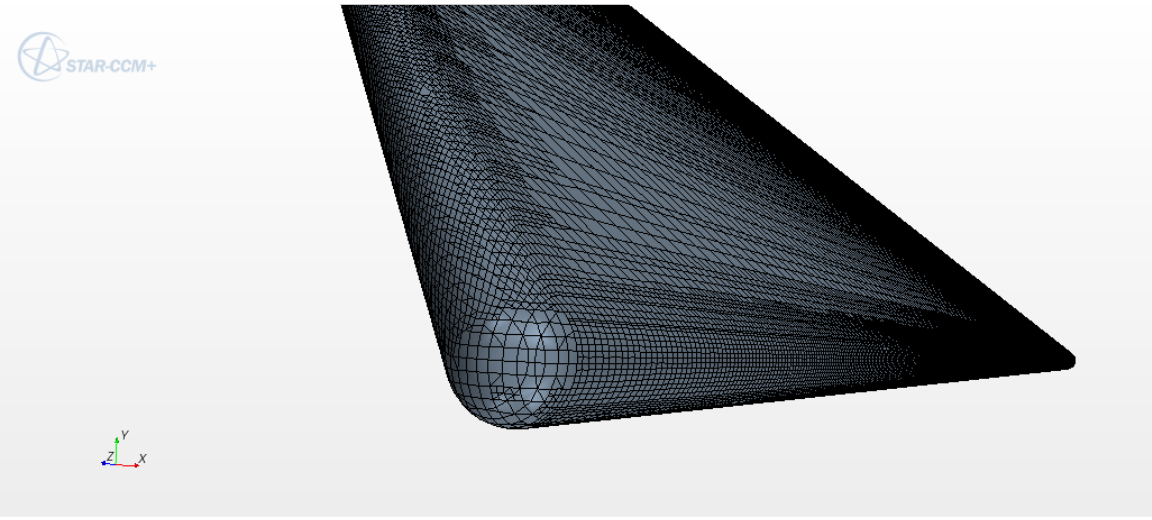

Figure 7.2. Representative surface mesh near the edges and corners of the DWVG

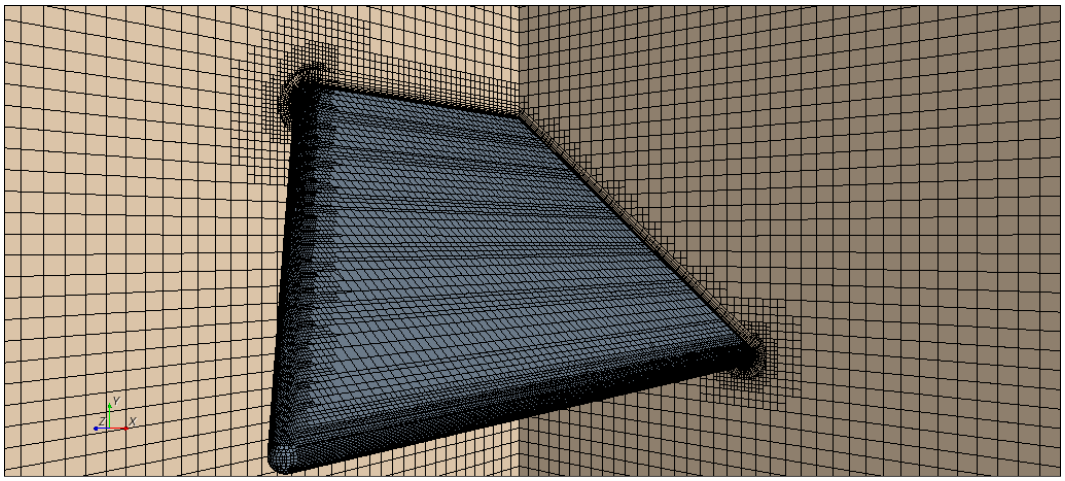

Figure 7.3. Representative volume mesh near DWVG for grid 3

7.2 Velocity Vector and Streamline Results

Comparisons of the velocity vectors in the region just off the trailing edge of the vortex generator were generated as a means of qualitatively investigating the vertical mixing as well as for comparison between the three levels of mesh refinement described in the previous section. Streamlines were also generated in order to investigate vertical mixing, as well indentify in an approximate fashion the path that algae might conceivably travel in these channels. These results are again only given for the 3.5 DWW case as this was the sole case for which comparison between meshes is available. Additionally, the velocity vector and streamline results are not an effective means of making comparisons between the different spacings studied, as they are very qualitative in nature. However the results given here were typical of those for all the simulations.

Figures 7.4-a through c show the in-plane velocity vectors colored by the vertical component of velocity for grids 1, 2, and 3 respectively. There is excellent agreement between all three grids both in terms of a qualitative comparison of the vectors as well as the range of vertical velocity in the plane shown.

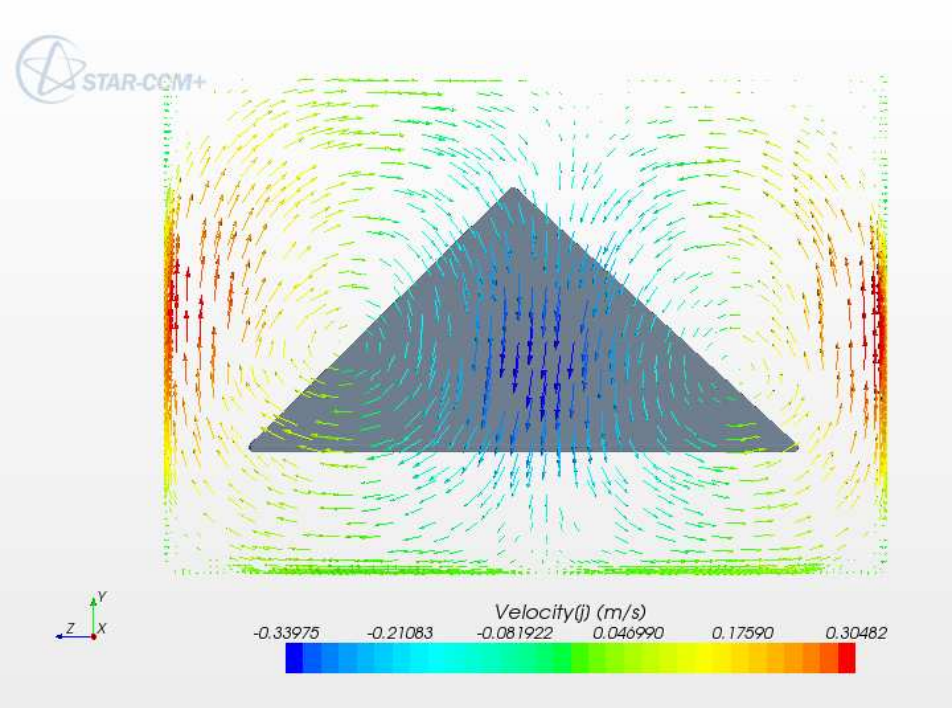

Figure 7.4-a. Plot of velocity vectors colored by the vertical velocity for plane just off trailing edge of the DWVG for grid 1 of the 3.5 DWW spacing

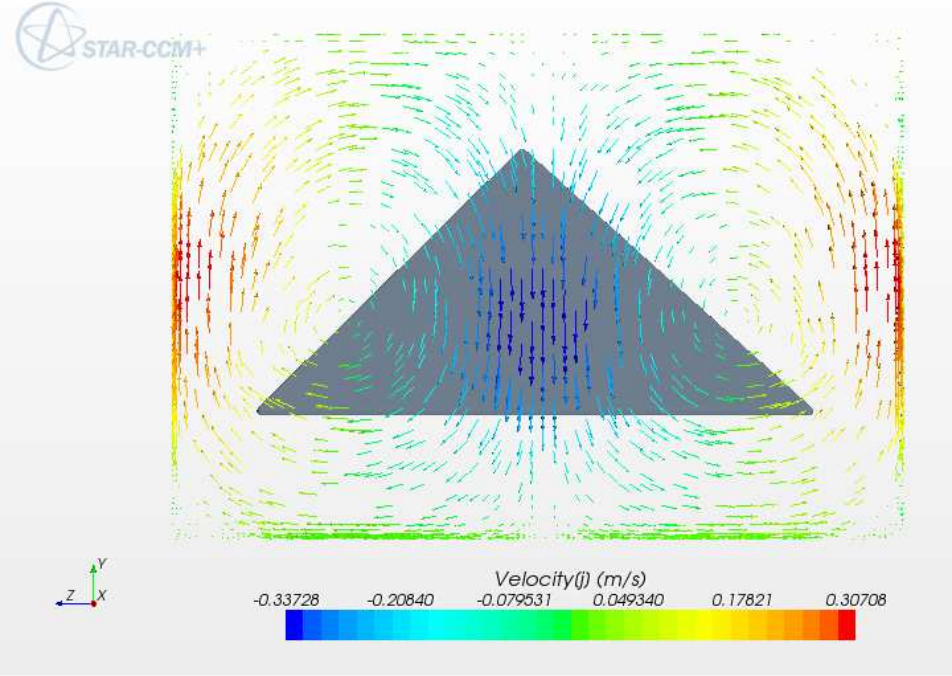

Figure 7.4-b. Plot of velocity vectors colored by the vertical velocity for plane just off trailing edge of the DWVG for grid 2 of the 3.5 DWW spacing

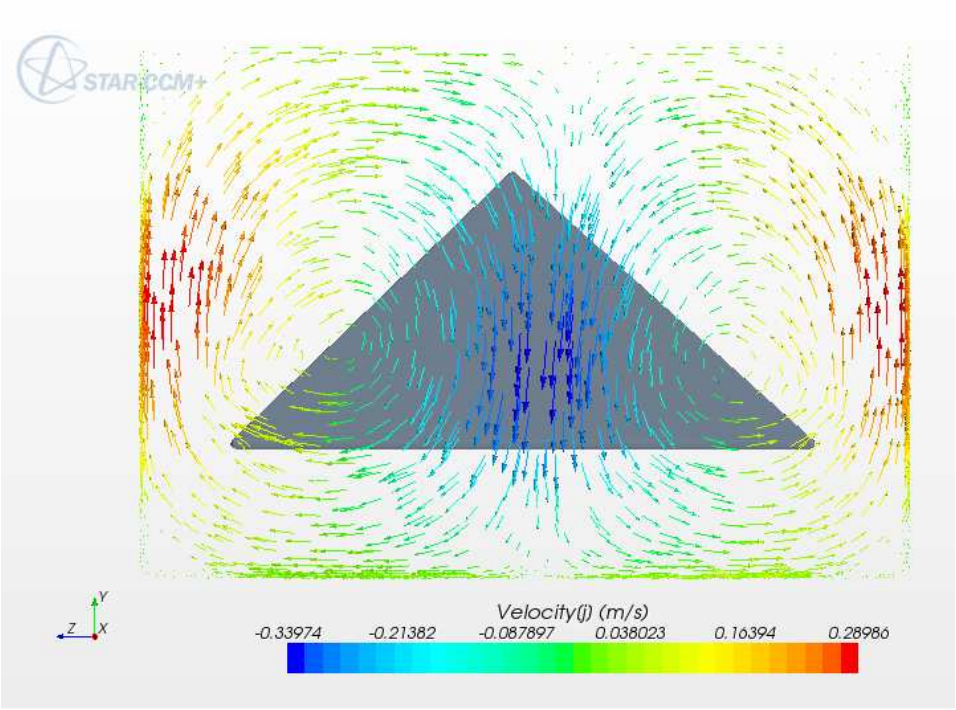

Figure 7.4-c. Plot of velocity vectors colored by the vertical velocity for plane just off trailing edge of the DWVG for grid 3 of the 3.5 DWW spacing

Additionally, these vector plots are instructive as they clearly indicate that the CFD simulations capture the LSVs described in Chapter 2. A pair of vortices form on either side of the DWVG, combined these vortices occupy the full width and height of the channel. It is also apparent that these vortices would have the impact of cycling the resident algae between the upper and lower extents of the raceway. This motion is precisely the desired outcome of vortex generation in this application.

A more precise view of the path traveled by algae in a channel segment equipped with DWVGs is available by plotting the streamlines. Though the flow is unsteady and consequently streamlines are not identical with pathlines, they will still provide a very good approximation to the path traveled. Figure 7.5 shows the streamlines for the fine grid; coloring is again by vertical velocity component.

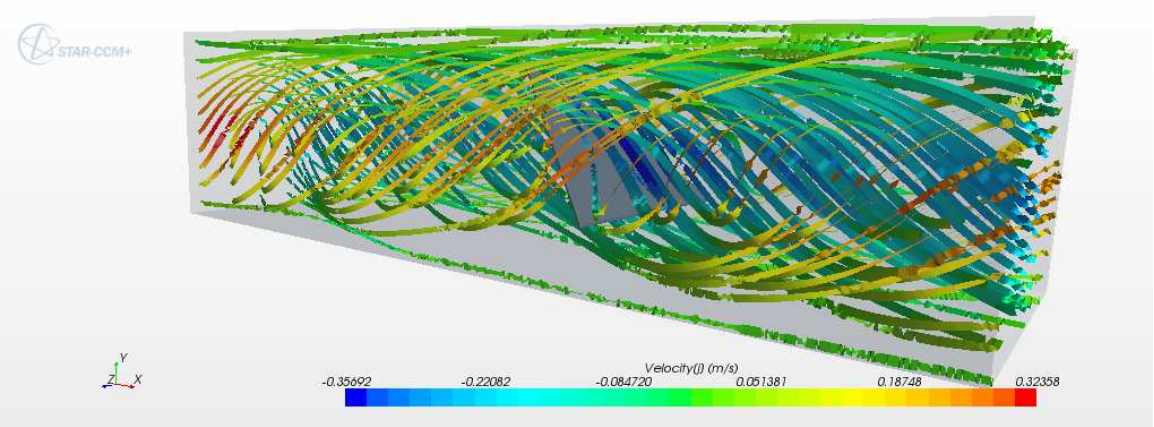

Figure 7.5. Streamlines colored by vertical velocity component for grid 3 of the 3.5 DWW spacing

This figure clearly demonstrates the presence of significant vertical motion. Algae present in such a raceway will have substantially more frequent exposure to the light rich surface than algae in traditional raceways.

7.3 Vertical Mixing Intensity Results

The above reported results are very encouraging and confirm the hypothesis developed following the complete raceway simulation, namely, that a series of DWVGs could cause significant amounts of vertical mixing. This knowledge however, is incomplete without an exact quantification of vertical mixing, and an understanding of the impact that spacing and angle of attack have on this value. Vertical mixing intensity as defined in Eqn. (12) is used to quantify the results and below is shown versus spacing in Fig. 7.6 and angle of attack in Fig. 7.7.

These figures illustrate several important points. First, the relationships between vertical mixing and spacing and angle of attack follow a trend that we would largely have expected. Namely, that shorter spacing increase vertical mixing while smaller angles of attack decrease it. However, if we look at the range of vertical mixing intensities present

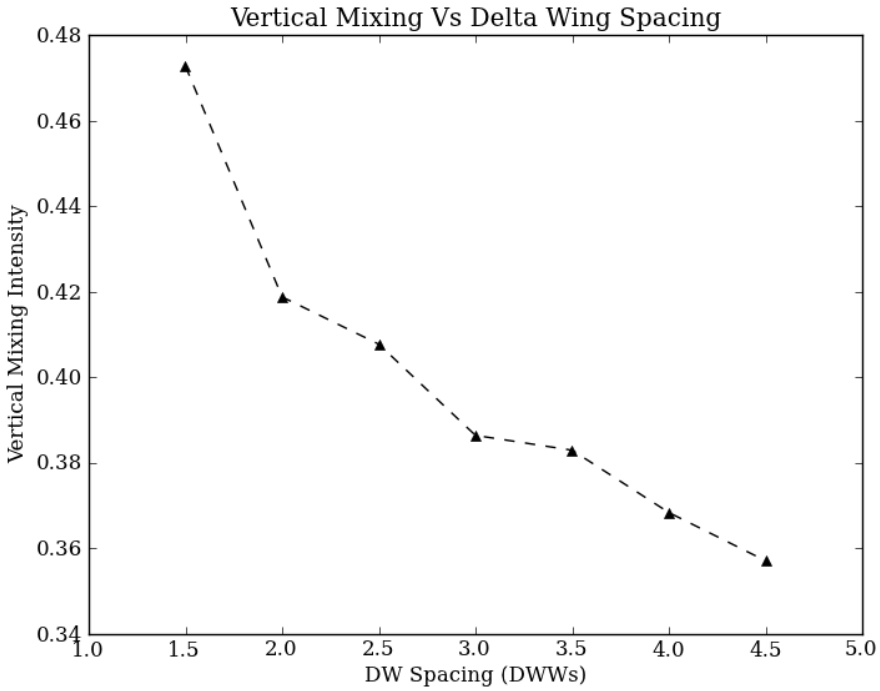

Figure 7.6. Vertical mixing intensity versus DWVG spacing

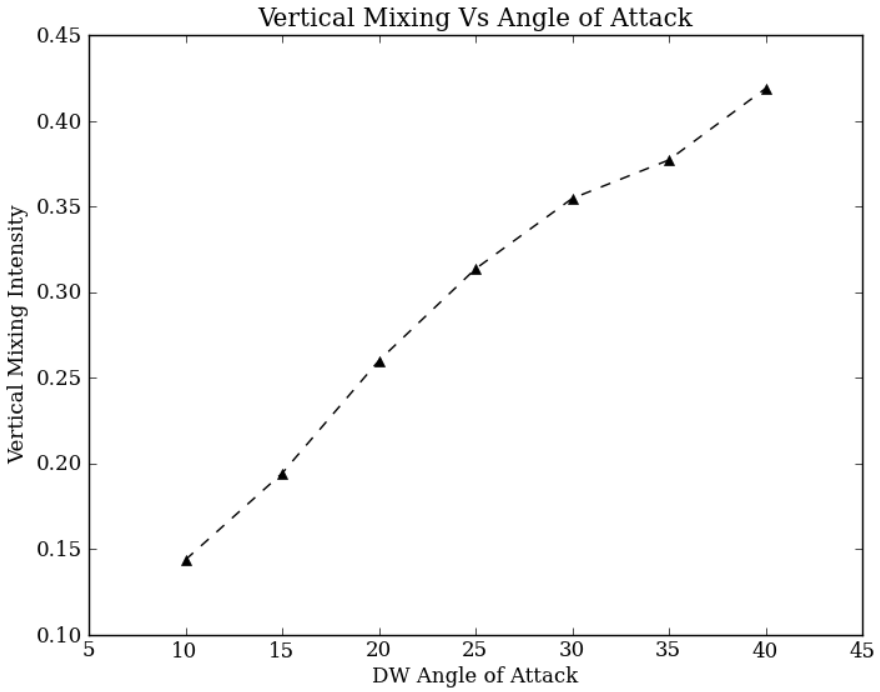

Figure 7.7. Vertical mixing intensity versus DWVG angle of attack

in both sets of experiments it is clear that changes in angle of attack have a larger impact on vertical mixing than do changes in spacing. In fact, the maximum difference between mixing intensities as a percentage of the highest mixing in their respective experiments is 65% for the angle of attack experiment and only 24% for the spacing experiment.

It further appears from Fig. 7.6 vertical mixing decreases in a non-linear fashion with spacing. Such that additional increases in spacing may be expected to have smaller and smaller impacts on vertical mixing. Conversely, vertical mixing appears to increase linearly with angle of attack. These observations indicate that more attention should be given to the angle of attack when seeking to optimize a raceway.

7.4 Mass Specific Power Requirement Results

As stated in Chapter 6, the increase in power requirement due to the addition of a series of DWVGs is an essential piece of information for the current application. Significant increases in the power required to run a raceway would rule out successful implementation of this technology. Thus, for viability a configuration that establishes the vertical mixing reported on the previous two sections must come with a minimal increase in power requirement. Both sets of experiments were used to determine the impact of their respective independent variables on the mass specific power requirement computed as outlined in Chapter 6. Figs. 7.8 and 7.9 below show the results of these experiments as functions of spacing and angle of attack, respectively.

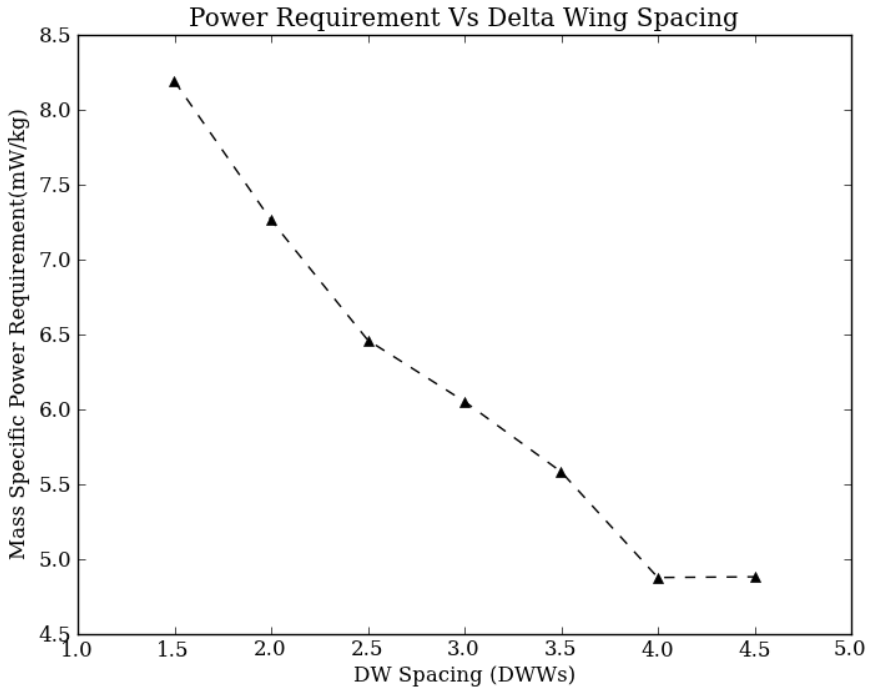

Figure 7.8. Mass specific power requirement versus DWVG spacing

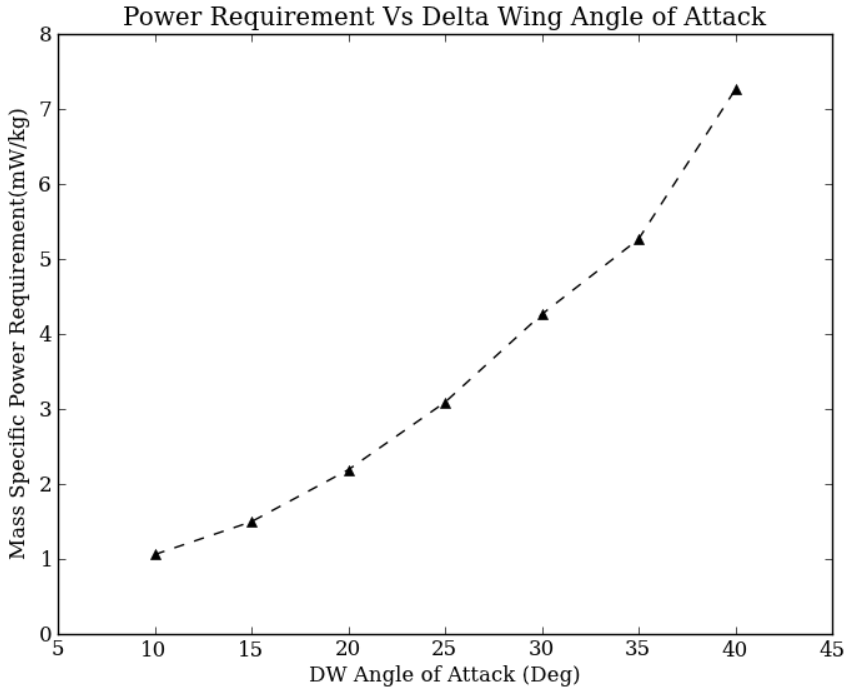

Figure 7.9. Mass specific power requirement versus DWVG angle of attack

The same general trend as was seen in section 7.3 is displayed here as well. Increases in spacing are shown to decrease the independent variable, while increases in angle of attack increase it (power requirement). Just as before these trends are precisely what we would expect. A second pattern that was shown before is that angle of attack appears to have a greater impact that spacing on the power requirement; however, in this case the relationship appears to be nonlinear. Spacing appears to be characterized by a more or less inverse linear relationship, with the exception of the final data point, which counterintuitively showed a very slight increase in mass specific power requirement over the next smaller spacing. Inspection of Fig. 7.6 shows that there is no perceivable anomaly in the results on vertical mixing.

Combining the results presented in this section with those of the last section allows investigation of an optimum configuration from the stand point of maximizing vertical mixing intensity while decreasing mass specific power requirement. Figs. 7.10 and 7.11 are plots of the vertical mixing intensity divided by the mass specific power requirement for the spacing and angle of attack experiments respectively. A higher number indicates a more desirable ratio of mixing to power requirement.

Both of these figures illustrate that either shorter spacings or higher angles of attack result in a decreased vertical mixing to power ratio. The significance of this is that configurations designed to generate the most intense vertical mixing will not only consume more power but will consume it in a less efficient manner. This implies that care should be taken to operate algal cultivation raceways at the lowest level of vertical mixing that sufficiently stimulates algae growth.

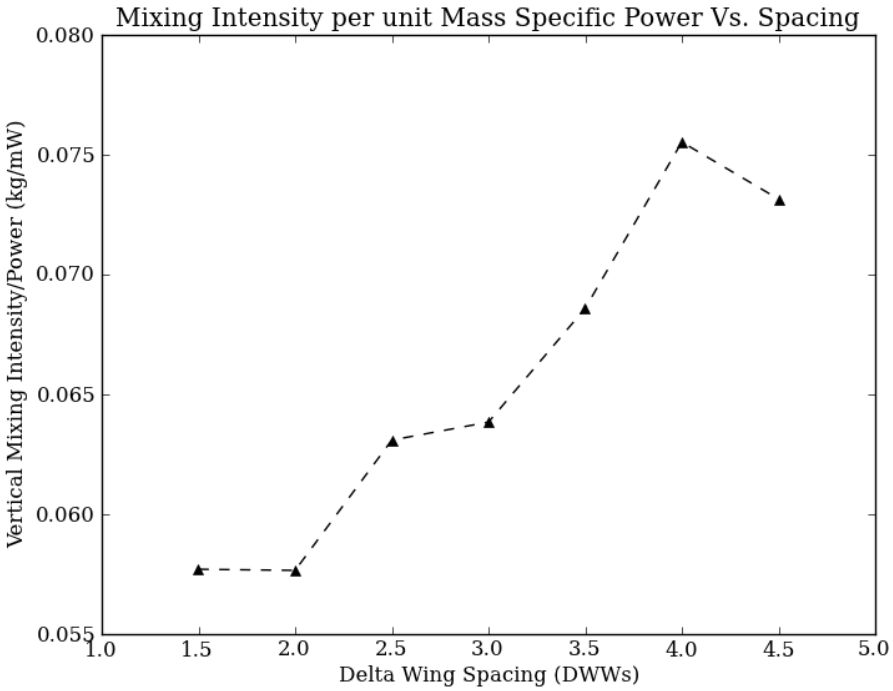

Figure 7.10. Ratio of vertical mixing to power requirement versus DWVG spacing

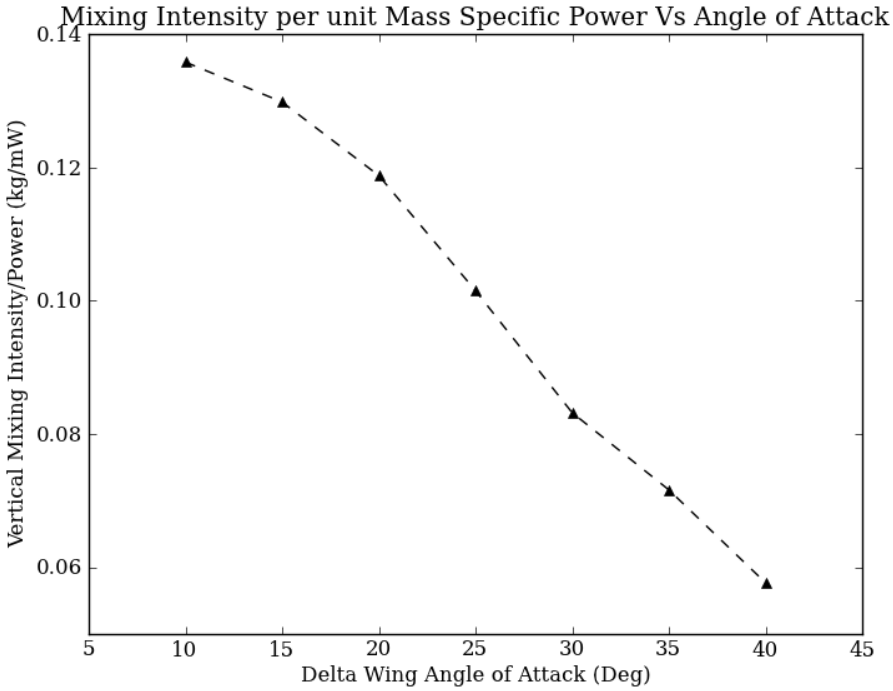

Figure 7.11. Ratio of vertical mixing to power requirement versus DWVG angle of attack

7.5 Discussion

The contents of this chapter have demonstrated that significant levels of vertical mixing are generated by the presence of a series of DWVGs in channel segments. Additionally, it is clear that the type of motion present is ideal for the cycling of algae between the upper and lower extents of a raceway. System power requirements were also investigated, and the relationship between both spacing and angle of attack was shown. These results indicated that the most efficient systems from the perspective of the power requirement are those that seek to generate vertical mixing on the lower end of those studied.

CHAPTER 8

CONCLUSIONS AND FURTHER WORK

The work contained in this thesis undertook to thoroughly investigate the potential of DWVGs to generate vertical mixing in algae cultivation raceways in an economical manner.

From resulting CFD work it can be concluded that for meaningful increases in vertical mixing a series of DWVGs is required. This was the result of contradictory mixing time analysis comparing a raceway with no DWVGs with one containing a single generator in each channel. Analysis of the velocity vectors in the region of the DWs however, clearly demonstrated that at least in their immediate vicinity DWVGs will generate vertical circulation.

Additionally, the raceway simulations conclusively demonstrate that the hydrodynamic environments characteristic of algae raceways represent levels of turbulence significantly higher than those levels at which many species of algae have been shown to have decreased productivity. This should serve as evidence that turbulence sensitivity of the organism is likely to play a significant role in overall system productivity. The literature review showed that there are species of algae that can benefit from turbulence; it is possible that these species may be significantly more productive in raceway environments even when compared to species that demonstrate higher levels of lipid accumulation.

Further investigation into the potential of a series of DWVGs showed that very significant levels of vertical mixing can be maintained by such a configuration.

Maximum levels of vertical mixing were shown to result in an average vertical component of velocity that was 48% the average velocity determined by mass flow rate.

Additionally, while it was clearly demonstrated that both spacing and angle of attack played a role in the levels of mixing attained; it was also shown that the angle of attack represents a more significant means of controlling vertical mixing in a raceway than vortex generator spacing.

Finally it was shown that from the perspective of power efficiency more moderate levels of vertical mixing are ideal. The relationship between both spacing and angle of attack were shown to be such that configurations capable of generating the highest levels of vertical mixing were the least efficient in terms of power requirement. The implication that this has for raceway design is that care should be maintained to generate the lowest amount of mixing that can be shown to be effective. Unfortunately, this level cannot be determined solely from the work contained herein, as it is primarily a function of algae productivity.

This thought is the first indication of the potential for future work on this technology. Given the strong evidence from a hydrodynamic perspective that DWVGs represent a viable technology for increasing vertical mixing, it remains to be shown if the biological side of the question responds as favorably. For true success it must be demonstrated that algae cultures will indeed react favorable to the environments shown to be generated by DWVGs. Experimentation that seeks to answer this question is a potentially fruitful area of research. In particular, it would be valuable to understand the nature of algae response to vertical mixing. If positive, does it increase continually, or is

there a threshold value beyond which little to no improvement is noticed, or decreases are seen.

REFERENCES

[1] Bang, G., 2010, "Energy Security and Climate Change Concerns: Triggers for Energy Policy Change in the United States?," Energy Policy, 38(4), pp. 1645-1653.

[2] Stephens, E., Ross, I.A., Mussgnug, J.H., Wagner, L.D., Borowitzka, M.A., Posten, C., Kruse, O., and Hankamer B., 2010, "Future Prospects of Microalgal Biofuel Production Systems," Trends in Plant Sci., 15(10), pp. 554-564.

[3] Singh, J., and Gu, S., 2010, "Commercialization Potential of Microalgae for Biofuels Production," Renewable and Sustainable Energy Reviews, 14(9), pp. 2596-2610.

[4] Harun, R., Davidson, M., Doyle, M., Gopiraj, R., Danquah, M., and Forde, G., 2011, "Technoeconomic Analysis of an Integrated Microalgae Photobioreactor, Biodiesel and Biogas Production Facility," Biomass and Bioenergy, 35(1), pp. 747-747.

[5] Gallagher, B.J., 2011, "The Economics of Producing Biodiesel from Algae," Renewable Energy, 36(1), pp. 158-162.

[6] Mata, T.M., Martins, A.A., and Caetano, N.S., 2010, "Microalgae for Biodiesel Production and Other Applications: A Review," Renewable and Sustainable Energy Reviews, 14(1), pp. 217-232.

[7] Christenson, L., and Sims, R., 2011, "Production and Harvesting of Microalgae for Wastewater Treatment, Biofuels, and Bioproducts," Biotechnol. Advances, 29(6), pp. 686-702.

[8] Uduman, Y., Qi, Y., Danquah, M.K., Forde, G., and Hoadley, A., 2010, "Dewatering of Microalgal Cultures: A Major Bottleneck to Algae-Based Fuels," J. Renewable and Sustainable Energy, 2(1), pp. 1-16.

[9] Tuttle, R.C., and Loeblich, A.R., 1975, “An Optimal Growth Medium for the Dinoflagellate Crypthecodinium Cohnii,” Phycologia, 14(1), pp. 1-8.

[10] Powell, T.M., Richerson P.J., Dillon, T.M., Agee, B.A., Dozier, B.J., Godden D.A., and Myrup, L.O., 1975, “Spatial Scales of Current Speed and Hytoplankton Biomass Fluctuations in Lake Tahoe,” Science, 189(4208), pp. 1088-1090.

[11] White, A.W., 1976, “Growth-Inhibition Caused by Turbulence in the Toxic Marine Dinoflagellate Gonyaulax-Excavata,” J. Fisheries Res. Board of Canada, 33(11), pp. 2598-2602.

[12] Pollingher, U., and Zemel, E., 1981, “In Situ and Experimental Evidence of the Influence of Turbulence on Cell Division Processes of Peridinium Cinctum Forma Westii (Lemm.) Lefèvre,” British Phycological J., 16(3), pp. 281-287.

[13] Thomas, W.H., and Gibson, C.H., 1992, “Effects of Quantified Small-Scale Turbulence on the Dinoflagellate, Gymnodium Sanguineum (Splendens): Contrasts with Gonyaulax (Lingulodinium) Polyedra, and the Fishery Implication,” Deep Sea Research Part A. Oceanographic Res. Papers, 39(7-8), pp. 1429-1437.

[14] Hondzo, M., Kapur, A., and Lembi, C.A., 1997, “The Effect of Small-Scale Fluid Motion on the Green Alga Scenedesmus Quadricauda,” Hydrobiologia, 364(2), pp. 225-235.

[15] Sullivan, J.M., and Swift, E., 2003, “Effects of Small-Scale Turbulence on Net Growth Rate and Size of Ten Species of Marine Dinoflagellages,” J. Phycology, 39(1), pp. 83-94.

[16] Warnaars, T.A., and Hondzo, M., 2006, "Small-Scale Fluid Motion Mediates Growth and Nutrient Uptake of Selenastrum Capricornutum," Freshwater Biology, 51(6), pp. 999-1015.

[17] Fiebig, M., Kallweit, P., Mitra, N., and Tiggelbeck, S., 1991, "Heat-Transfer Enhancement and Drag by Longitudinal Vortex Generators in Channel Flow," Experimental Thermal and Fluid Science, 4(1), pp. 103-114.

[18] Tiggelbeck, S., Mitra, N.K., and Fiebig, M, 1994, "Comparison of Wing-Type Vortex Generators for Heat-Transfer Enhancement," J. Heat Transfer-Trans. ASME, 116(4), pp. 880-885.

[19] Biswas, G., Torii, K.. Fujii, D., and Nishino, K., 1996, "Numerical and Experimental Determination of Flow Structure and Heat Transfer Effects of Longitudinal Vortices in a Channel Flow," Intl. J. Heat and Mass Transfer, 39(16), pp. 3441-3451.

[20] Gentry, M.C., and Jacobi, A.M., 2002, "Heat Transfer Enhancement by Delta-Wing-Generated Tip Vortices in Flat-Plate and Developing Channel Flows," J. Heat Transfer, 124(6), pp. 1158-1168.

[21] Eibeck, P.A., and Eaton, J.K., 1987, "Heat Transfer Effects of a Longitudinal Vortex Embedded in a Turbulent Shear Flow," J. Heat Transfer, 109(1), pp. 16-24.

[22] Versteeg, H.K., and Malalasekera, W., 2007, *An Introduction to Computational Fluid Dynamics: The Finite Volume Method*, 2nd ed., Prentice Hall, Essex, England, Chap. 3.

[23] Ansys Fluent Theory Manual 12.0, 2009.

[24] User Guide Star CCM+ Version 6.06.11, 2011.

[25] Haque A. U., Khawar, J., and Ch, S.R., 2008, "Influence of Turbulence Modeling in Capturing Separated Flow Over Delta Wing at Subsonic Speed," Engineering Applications of Computational Fluid Mechanics, 2(), pp. 252-263.

[26] Wilcox, D.C., 1994, *Turbulence Modeling for CFD*, 2nd ed., DCW Industries, La Canada, California.

[27] Spall, R., Jones, N., and Staheli, C., 2010, "Computational Fluid Dynamics Analysis of Fluid Mixing in Single Use Bioreactors," *International Mechanical Engineering Congress and Exposition*, American Society of Mechanical Engineers, Vancouver, British Columbia.

[28] Celik, I.B., Ghia, U., Roache, P.J., and Freitas, C., "Procedure for Estimation and Reporting of Uncertainty Due to Discretization in CFD Applications," J. Fluids Engineering Editorial Policy Statement on the Control of Numerical Accuracy.

APPENDIX

Appropriate modeling requires the identification of all the relevant dimensionless parameters. This appendix includes a proposed set of dimensionless parameters identified by means of the Buckingham Pi Theorem. The details of the work are not included, only the parameters themselves. In particular power requirement in the straight channel segments reported on in Chapter 7 was investigated. Equation 13 below shows the relationship that was defined between the dimensionless power and the Pi's.

$$\frac{P_s A_{dw}^{7/2}}{Q^3} = f\left(\frac{1}{\mathrm{Re}_{dw}}, \alpha, \frac{s}{\sqrt{A_{dw}}}\right) \tag{13}$$

where A_{dw} is the surface area of the DWVG, Q is the volumetric flow rate, α is the DWVG angle of attack, s is the DWVG spacing and Re_{dw} is the Reynolds number based on the DWVG the equation for which is given in Eqn. 14 below.

$$\mathrm{Re}_{dw} = \frac{Q}{\nu\sqrt{A_{dw}}} \tag{14}$$

where ν is the fluid kinematic viscosity.